Available online at www.sciencedirect.com
SCIENCE DIRECT®
Ecological Modelling 187 (2005) 140–178
ECOLOGICAL MODELLING
www.elsevier.com/locate/ecolmodel

Eutrophication model for Lake Washington (USA) Part I. Model description and sensitivity analysis

George B. Arhonditsis*, Michael T. Brett

Department of Civil and Environmental Engineering, University of Washington, P.O. Box 352700, Seattle, WA 98195, USA

Received 7 April 2004; received in revised form 8 January 2005; accepted 17 January 2005
Available online 3 March 2005

Abstract

Complex environmental models are often criticized as being difficult to analyze and poorly identifiable due to their nonlinearities and/or their large number of parameters relative to data availability. Others consider overparameterized models to be useful, especially for predicting system dynamics beyond the conditions for which the model was calibrated. In this paper, we present a complex eutrophication model that has been developed to simulate plankton dynamics in Lake Washington, USA. Because this model is to be used for testing alternative managerial schemes, the inclusion of multiple elemental cycles (org. C, N, P, Si, O) and multiple functional phytoplankton (diatoms, green algae and cyanobacteria) and zooplankton (copepods and cladocerans) groups was deemed necessary. The model also takes into account recent advances in stoichiometric nutrient recycling theory, and the zooplankton grazing term was reformulated to include algal food quality effects on zooplankton assimilation efficiency. The physical structure of the model is simple and consists of two spatial compartments representing the lake epilimnion and hypolimnion. Global sensitivity analysis showed background light attenuation, the maximum phytoplankton growth rate, the phytoplankton basal metabolic rate, the zooplankton maximum grazing rate and the grazing half saturation constant have the greatest impact on model behavior. Phytoplankton phosphorus stoichiometry (maximum and minimum internal concentrations, maximum uptake rate) interacts with these parameters and determines the plankton dynamics (epilimnetic and hypolimnetic phytoplankton biomass, proportion of cyanobacteria and total zooplankton biomass). Sensitivity analysis of the model forcing functions indicated the importance of both external and internal loading for simulating epilimnetic and hypolimnetic plankton dynamics. These results will be used to calibrate the model, to reproduce present chemical and biological properties of Lake Washington and to test this lake's potential response to different external nutrient loading scenarios.
© 2005 Elsevier B.V. All rights reserved.

Keywords: Eutrophication; Lake Washington; Plankton dynamics; Stoichiometric theory

1. Introduction

Classical modeling approaches for addressing lake eutrophication are based mostly on Vollenweider's (1975) and Dillon and Rigler (1974) steady-state,

* Corresponding author. Present address: Nicholas School of the Environment and Earth Sciences, Duke University, Durham, NC, USA. Tel.: +1 919 613 8105; fax: +1 919 681 5740.
E-mail address: georgear@duke.edu (G.B. Arhonditsis).

0304-3800/$ – see front matter © 2005 Elsevier B.V. All rights reserved.
doi:10.1016/j.ecolmodel.2005.01.040

input–output equations. These mass-balance models predict lake total phosphorus (TP) concentrations based on TP input concentrations, phosphorus retention in the sediments, and lake hydrologic retention times, and these predicted TP concentrations are in turn associated with phytoplankton biomass indicators such as chlorophyll a concentrations (see also, review by Ahlgren et al., 1988; Meeuwig and Peters, 1996). An alternative to these "data-oriented" models is "process-oriented" water quality models, which have a more explicit mechanistic basis and include chemical/biological interactions usually not taken into account in mass balance models (Jorgensen, 1997; Reckhow and Chapra, 1999). Conceptually, these mechanistic models summarize the state of knowledge in limnology, and can be extrapolated to similar systems and used to predict responses to nutrient enrichment scenarios (Omlin et al., 2001b). Significant progress in the development and application of mechanistic lake water quality models has occurred during the last two decades (Riley and Stefan, 1988; Karagounis et al., 1993; Cole and Buchak, 1995; Hamilton and Schladow, 1997; Omlin et al., 2001a; Chen et al., 2002). Most of these plankton models have been coupled with hydrodynamic models and include detailed biogeochemical/biological processes that allow for comprehensive assessments of system behavior under a wide variety of conditions. In addition, recent advancements in lake modeling involve very promising structural dynamic approaches that use goal functions, derived from non-equilibrium thermodynamics (e.g., exergy; see Jorgensen, 1999), to track the direction of ecosystem development (Jorgensen et al., 2002; Zhang et al., 2003a,b, 2004).

In practice, however, the basic premise of mechanistic water quality simulation models, i.e., the causal description of the internal system structure based on current scientific understanding, is also their main source of criticism as many scientists deem these models overparameterized constructs that violate the parsimony principle (Beck, 1987). Modelers challenged by the enormous complexity of ecological systems or driven by the need to include processes that could become important in hypothesized future states, develop complex and poorly identifiable models (Brun et al., 2001). Hence, identifiability analysis (model structure selection, parameter identification) is a "thorny" issue for this class of models and as such has often been debated (Beck, 1987; Janssen, 1994; Klepper, 1997; Brun et al., 2001). The nature of the parameter identification problem when using large and complex environmental models was clearly stated by Klepper (1997) and Brun et al. (2001). It was argued that there is no point in requiring rigorous identifiability in this class of models and that existing data will rarely provide unique estimates of many of the model parameters. In this context, a reasonable objective is to find "physically reasonable parameter values" that adequately describe general trends in the data, and to apply sensitivity analysis that make it possible to unravel the most important parameters, and recognize parameter interaction patterns in order to gain insights about model behavior (Brun et al., 2001).

By evaluating a mechanistic eutrophication model, Hornberger and Spear (1980) introduced a regional approach that a priori discriminates between areas of acceptable and unacceptable model performance and then explores the parameter space for physically reasonable values through various sampling schemes (i.e., Monte Carlo simulations). While recent improvements have increased the efficacy of this algorithm (Spear, 1997), regional sensitivity analysis still has severe difficulties in scrutinizing multidimensional parameter spaces because only a small proportion of the parameter combinations used result in acceptable model performance. An alternative method is the local sensitivity analysis which, instead of varying the parameters over a priori determined ranges, works with the model output derivatives with respect to the parameters at a specific point of the parameter space (Beck, 1987). This approach seems to be particularly effective when prior knowledge of parameter values can be associated with reasonable model performance (Brun et al., 2001), and interesting eutrophication applications were presented by Pastres et al. (1997) and Omlin et al. (2001b). The former study performed a first-order local sensitivity analysis in a 1D reaction-diffusion model, which pointed out the reciprocal relation between diffusivity and kinetic parameter identifiability and tuning importance. The latter study used a 1D biogeochemical model for Lake Zurich and methods introduced by Brun et al. (2001), based on prior estimates of parameter uncertainty and linear propagation techniques, to determine the influence of several parameters (e.g., half-saturation light intensity of algal growth) and indicate the non-identifiability problems between parameters

relevant to algal and zooplankton growth, respiration and death. Water quality simulation models have also been combined with global sensitivity analysis techniques, which are useful for evaluating average parameter effects on model sensitivity with Monte Carlo sampling over the entire parameter space (Helton, 1993; Heuberger and Janssen, 1994). For example, interesting insights on system dynamics and data parameterizations were found by Campolongo and Saltelli (1997), who used a phytoplankton-dimethylsulphide production model to compare various sensitivity analysis indicators (i.e., standardized regression coefficients, Morris and Sobol' indices) and tested their accuracy with bootstrap methods. Finally, an illustrative application on a shallow-water 3D eutrophication model based on Sobol' and linear regression methods was provided by Pastres et al. (1999).

In this paper, we present process formulations and sensitivity analysis for a complex eutrophication model for Lake Washington, USA. The model was developed as part of a long-term study and will ultimately be a component of an integrated series of hydrodynamic and fish-bioenergetic models. This model simulates five elemental cycles (org. C, N, P, Si, O) as well as three phytoplankton (diatoms, green algae and cyanobacteria) and two zooplankton (copepods and cladocerans) groups. We explicitly consider the interplay between the mass balance of multiple chemical elements and trophic dynamics (Elser and Urabe, 1999). Global sensitivity analysis is used as an initial screening test to identify the most influential model parameters, which then through a more regional approach are quantitatively assessed in terms of their relative impacts on the spatio-temporal outputs of the model. Plankton stoichiometries are separately processed, but their interactions with the kinetic parameters are also considered. Finally, we evaluate the influence of forcing function uncertainties (water temperature, solar radiation, diffusivity values, epilimnion depth, external and internal nutrient loading) on the model results.

2. Description of the model

This section describes the basic conceptual design of the model. The differential equations are presented in Appendix A, while the symbols and parameter definitions are presented in Appendix B. Some of the model parameterizations are quite common and have been well documented in the modeling literature, so we will only briefly describe them. We will emphasize special features of the model and site-specific modifications for Lake Washington.

2.1. Model spatial structure and forcing functions

As previously mentioned, the present modeling study is one component of an integrated approach and will be combined with a hydrodynamic and a fish bioenergetics model. At this point, we present the eutrophication model within a simple physical segmentation (Fig. 1), which considers a two-compartment vertical system representing the epilimnion and hypolimnion of the lake (see review by Rajar and Cetina, 1997).

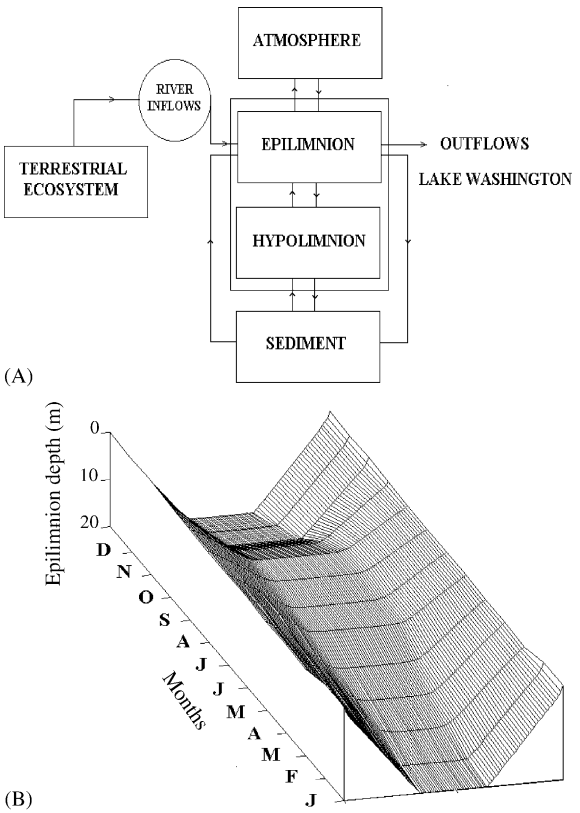

Fig. 1. (A) The flow diagram of the biological submodel, consisting of two spatial compartments (epilimnion and hypolimnion). (B) Annual variability of the epilimnion compartment, based on the trapezoidal spatial structure of the model. Note that the used structure allows for sediment–water exchanges in the epilimnion.

This simplified approach is probably insufficient and a multiple-layer vertical characterization of the system would be more appropriate for comprehending the system's dynamics (Hamilton and Schladow, 1997). This is particularly important during the initiation of the spring bloom and the subsequent summer stratified period when interactions between physical and chemical/biological processes can cause structural shifts in the phytoplankton community (see also Arhonditsis and Brett, Part II). In contrast, the information that is lost by not considering heterogeneity over the horizontal plane does not seem to be restrictive for understanding the present system. Statistical analysis of the current spatial and temporal patterns for the epilimnion of Lake Washington showed that seasonal fluctuations explained 40% of the total variability for the major water quality parameters, spatial heterogeneity explained 10%, and seasonal–spatial interactions explained 10% of this variability (Arhonditsis et al., 2003). The spatial discontinuities are mostly due to differences in pH, nitrate and phosphate levels between inshore and offshore sections of the lake, which in turn were attributed to differences in bicarbonate system equilibrium dynamics between shallow and deep regions of the lake and the lower nutrient levels in the southern end of the lake due to the dilution effects of discharges from the nutrient-poor Cedar River (Arhonditsis et al., 2003). Nonetheless, the influence of this heterogeneity on the system's phytoplankton and zooplankton dynamics was small. For example, the phytoplankton biomass increases uniformly during the spring bloom, while no general and consistent patterns exist in terms of the horizontal distribution of the zooplankton populations (Edmondson and Litt, 1982; Arhonditsis et al., 2003).

The depths of the two boxes varied with time and were explicitly defined based on extensive field measurements for the study period 1994–2000. During the stratified period, the epilimnion was defined as the maximum depth where the water temperature varied $\leq 1\,^{\circ}\mathrm{C}$ relative to the temperature at 0.5 m; otherwise, we assumed a box-depth of 20 m to reproduce patterns of incomplete mixing that regulate the ecological processes in the lake during the early spring (Arhonditsis et al., 2004b). Mass exchanges between the two compartments were computed using Fick's Law:

$$\mathrm{EPI/YPO}_{(\text{state variable})} = -\frac{1}{V_{(x)}(t)}\left\{A_z(t)\left[K(t)\frac{\Delta(\text{state variable})}{\Delta z}\right]\right\}$$

where $V_{(x)}(t)$ is the epilimnion or hypolimnion volume (m^3); $K(t)$ the molecular plus the eddy diffusion coefficients ($m^2\ day^{-1}$); $A_z(t)$ the area at the depth z (m^2), the interface between the lake epilimnion–hypolimnion; and $\Delta(\text{state variable})/\Delta z$ the gradient between the centers of the two boxes for each of the state variables of the model. Values for the vertical diffusion coefficients were derived from measurements taken in past studies of this lake (Lehman, 1978; Walters, 1980; Quay et al., 1980).

The external forcing functions for the model were epilimnion and hypolimnion water temperatures, solar radiation, precipitation, river inflows and associated nutrient loading. Sinusoidal functions were used to approximate epilimnion ($r^2 = 0.99$) and hypolimnion ($r^2 = 0.98$) water temperatures and solar radiation ($r^2 = 0.99$) mean annual cycles, based on field measurements (Edmondson, 1997) and meteorological data from the SeaTac Airport weather station (47°45′N–122°30′W and 137 m), respectively. The mean annual external nutrient loading cycle was based on flow-weighted nutrient concentrations over the past 10 years for all the important Lake Washington tributaries (Brett et al., in press). Precipitation data, river inflows, evaporation estimates (Arhonditsis et al., 2004a), and outflow data from the H.H. Chittenden Locks of the Lake Union Ship Canal were used to run the model with the mean hydrologic cycle, while also accounting for lake volume variability. Finally, the effects of the simplified spatial structure (epilimnion depth and diffusivity values) along with uncertainty for the remaining forcing functions for model outputs will be tested through sensitivity analysis by inducing perturbations, based on the observed inter- and intra-annual variability (Section 3.4 and Part II).

2.2. Phytoplankton

The governing equation for algal biomass considers phytoplankton production and losses due to basal metabolism, settling and herbivorous zooplankton grazing. Nutrient, light and temperature impacts on phytoplankton growth are included using a multiplicative model (Cerco and Cole, 1994). Phosphorus and nitrogen dynamics within the phytoplankton cells account for luxury uptake (Hamilton and Schladow, 1997; Asaeda and Van Bon, 1997; Arhonditsis

et al., 2002), where phytoplankton nutrient uptake depends on both internal and external concentrations and is confined by upper and lower internal nutrient concentrations. The inorganic carbon required for algal growth is assumed to be in excess and thus is not considered by the model. Amongst the variety of mathematical formulations relating photosynthesis and light intensities, i.e., light saturation curves (see Jassby and Platt, 1976), we used Steele's equation with Beer's law to scale photosynthetically active radiation to depth. The extinction coefficient is determined as the sum of the background light attenuation and attenuation due to chlorophyll a, while the optimal illumination considers physiological adaptations by phytoplankton based on light levels during the two preceding model days (Ferris and Christian, 1991; Cerco and Cole, 1994). Phytoplankton growth temperature dependence has an optimum level and is modeled by a function similar to a Gaussian probability curve (Cerco and Cole, 1994). Phytoplankton basal metabolism includes all internal processes that decrease algal biomass (respiration, excretion) as well as natural mortality. Basal metabolism is assumed to increase exponentially with temperature.

An important property of eutrophication models is their ability to predict structural shifts in the phytoplankton community composition under different nutrient enrichment regimes. A detailed description of current phytoplankton seasonal successional patterns in Lake Washington was presented in Arhonditsis et al. (2003). Briefly, towards the end of the winter physical conditions become more favorable (increase of daylength, solar warming and a shallower mixed layer) and stimulate a substantial phytoplankton bloom during which chlorophyll a concentrations on average quadruple (i.e., from 2.5–10 $\mu g\, l^{-1}$). The spring bloom phytoplankton community is dominated by the diatoms (≈62%) *Aulacoseira*, *Stephanodiscus*, *Asterionella* and *Fragilaria*, and the chlorophytes (≈21%) *Actinastrum* and *Ankistrodesmus*, while cyanobacteria represent only a small fraction (≈8%). During the summer-stratified period, the chlorophyll concentrations vary from 2.5 to 3.5 $\mu g\, l^{-1}$ and the phytoplankton community is dominated by the chlorophytes (≈37%) *Oocystis* and *Sphaerocystis*, the diatoms (≈26%) *Aulacoseira* and *Fragilaria* and the cyanobacteria (≈25%) *Anabaena* and *Anacystis*. In its current recovered state, Lake Washington does not develop a significant fall phytoplankton bloom. The fall phytoplankton dynamics are driven by declining light availability and the progressive erosion and deepening of the metalimnion and approximate winter low levels (2–2.5 $\mu g\, l^{-1}$). Interestingly, cryptophytes comprise about 8% of the phytoplankton community throughout the year. Given these phytoplankton patterns, the first trophic level of the model distinguishes between three phytoplankton groups: diatoms, green algae and cyanobacteria. Similar discrimination of the phytoplankton assemblage was adopted in several recent studies (e.g., Asaeda and Van Bon, 1997; Menshutkin et al., 1998; Savchuk, 2002). The three phytoplankton groups differ in their maximum growth rates, nitrogen and phosphorus kinetics, light requirements, settling velocities, as well as feeding preference and food quality for herbivorous zooplankton. Diatoms are also distinguished by their silica requirements.

2.3. Zooplankton

There is an extensive literature that describes the community structure and dietary patterns of Lake Washington zooplankton (Edmondson and Litt, 1982; Infante and Edmondson, 1985). The sequence of species-specific peak abundances may change from one year to another, but the general succesional pattern can be summarized accordingly: the calanoid copepod *Leptodiaptomus ashlandi* is the dominant species during the winter and its seasonal maximum (usually late May) precedes that for *Daphnia* (*D. pulicaria*, *D. thorata*, *D. galeata mendotae*) which dominate the summer zooplankton. Other herbivorous zooplankton include *Diaphanosoma* (*D. birgei*) and *Ceriodaphnia*, but their densities are usually very low. Hence, the second trophic level (herbivory) of the model includes two functional groups, which are labeled as "copepods" and "cladocerans", and correspond to the general characteristics of a *Diaptomus* and *Daphnia*-like species, respectively. Furthermore, Lake Washington's omnivorous and carnivorous zooplankton do not appear to exert significant impacts on the two herbivores. For example, Edmondson and Litt (1982) report a rapid increase in *D. pulicaria* abundance during the peak abundance of the predaceous cladoceran *Leptodora kindtii*, while similar evidence for weak impacts exists for the carnivorous cyclopoid copepod *Cyclops bicuspidatus thomasi*. More significant appears to be the effect of

the calanoid *Epischura nevadensis*, which can persist at fairly high densities closely related with *Daphnia* and *Bosmina* (*B. longirostris*) abundance. In any event, zooplankton mortality due to consumption by omnivorous/carnivorous zooplankton seems to follow the physical driving forces, phytoplankton–zooplankton interactions, or alternatively to be the effect rather than the cause of zooplankton patterns in Lake Washington. Thus, possible inter-zooplankton effects were not explicitly modeled and along with predation by the mysid shrimp *Neomysis mercedis* are incorporated in the higher predation closure term.

The general characteristics of the two herbivores modeled include different temperature limitations, feeding rates, food preferences, selectivity strategies, stoichiometries and vulnerability to predators. These differences drive their successional patterns and their interactions with the phytoplankton community. Copepods have a wider temperature tolerance than daphnids, which allows copepods to dominate the winter zooplankton community and more promptly respond to the spring phytoplankton bloom. We also consider copepods to have higher feeding rates at low food abundance. In contrast, cladocerans become feeding saturated at higher food concentrations and consequently have a competitive advantage at greater food abundances (Muck and Lampert, 1984). Both groups graze phytoplankton and detritus but they differ greatly in their feeding selectivity. Cladocerans are filter-feeders with an equal preference between the four food-types (diatoms, green algae, cyanobacteria and detritus). Copepods are assumed to be capable of selecting on the basis of food quality and especially food particle size (DeMott, 1989). It should be noted that this description refers to the prior assigned preferences of the two zooplankton groups, which also change dynamically as a function of the relative proportion of the four food-types (Fasham et al., 1990). This means that the cladocerans select their food (equal nominal preferences) based on the respective abundance of the four food types, while copepod selection is determined through a more complex interaction between their ability to distinguish and actively ingest favorable food (different prior weights) at different food concentrations. Copepods have a slightly higher nitrogen and much lower phosphorus content compared to cladocerans (Andersen and Hessen, 1991), and their *C*:*N*:*P* ratios are nearly homeostatic over the annual cycle (Sterner and Hessen, 1994).

The choice of the higher predation closure term can have a strong influence on the dynamics of eutrophication models (Edwards and Yool, 2000). In addition, this choice has special importance in the present study since Lake Washington sockeye salmon (*Oncorhynchus nerka*) have some of the highest recorded juvenile growth rates for this species. Hence, they impose the highest consumption demands on *Daphnia* followed by rainbow trout (*Oncorhynchus mykiss*), yellow perch (*Perca flavescens*) and threespine sticklebacks (*Gasterosteus aculeatus*) (Beauchamp, 1996). Anson et al. (2002) reported a threshold of 0.4 ind l^{-1} (which usually occurs the end of May) as the level above which sockeye become strongly selective for *Daphnia* and avoid other prey taxa. The type of predation that is based on a prey threshold concentration is usually simulated by a sigmoid function (Malchow, 1994). In contrast, we have slightly relaxed this "switchable" type of predation for copepods and adopted a hyperbolic form (Fasham, 1993). When using the same half saturation constant with the 'S-shaped curve', the hyperbolic response leads to higher predation rates at low densities and the opposite when zooplankton are abundant. The former state corresponds to winter conditions when copepods dominate the zooplankton community, and the latter property was preferred (instead of a function that minimizes copepod predation during the summer) because the previously mentioned selective feeding is only described between sockeye salmon and *Daphnia* while zooplankton consumption patterns for other common fish in Lake Washington are not as well described.

A dynamic parameterization was used for modeling the effects of both ingested food quality and quantity on zooplankton gross growth efficiency (production: ingestion) (Straile, 1997; Brett and Müller-Navarra, 1997; Touratier et al., 2001). We used a hyperbolic formula (for example, see the conceptual diagram in Figure 4.28 of Lampert and Sommer, 1997) along with a variable that will be referred as "food quality concentration" (FQ) and is the product of two terms: (a) the first term is the sum of the square roots of the four food-type concentrations weighted by the respective qualities, expressed by a food quality index that varies from 0–1, and (b) the second term reflects the assumption

that the total food quality decreases by a factor directly proportional to the imbalance between the *C*:*P* ratio of the grazed seston and a critical $C{:}P_0$ ratio above which zooplankton growth will be limited by P availability. The weighting scheme of the first term considers differences in food quality other than the P content and accounts for biochemical/morphological characteristics of the four food-types. For example, it can characterize algal taxonomic differences in food quality due to differences in their highly unsaturated fatty acid, amino acid, protein content and/or digestibility (Ahlgren et al., 1990; Sterner and Hessen, 1994; Kilham et al., 1997; Kleppel et al., 1998; Müller-Navarra et al., 2000). This expression assumes that below the critical seston *C*:*P* threshold, the food concentration and biochemical composition solely determines zooplankton growth efficiency. Above the critical *C*:*P* threshold, mineral P limitation is an additional factor that influences food quality.

2.4. Biogeochemical cycles

We adopted a multi-elemental approach (organic carbon, nitrogen, phosphorus, silica and dissolved oxygen), which can be particularly useful for models that intend to make predictions and explore potential system dynamics outside of the calibration domain (Reichert and Omlin, 1997; Reckhow and Chapra, 1999). Most of the mechanistic information included in the model has quantitative – or at least qualitative – support, since Lake Washington has been intensively studied for over 40 years.

2.4.1. Organic carbon

Two carbon state variables are considered by the model: dissolved and particulate organic carbon (Fig. 2). Phytoplankton basal metabolism, zooplankton basal metabolism and egestion of excess carbon during zooplankton feeding release particulate and dis-

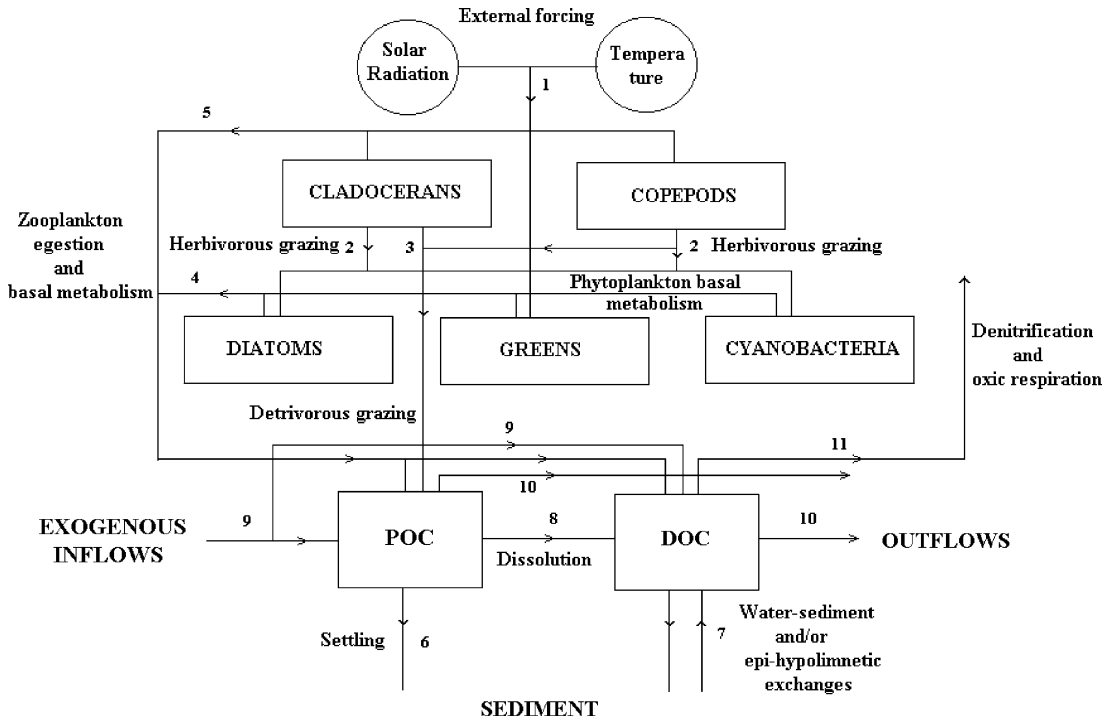

Fig. 2. The model carbon cycle: (1) external forcing to phytoplankton growth (temperature, solar radiation), (2) herbivorous grazing, (3) detrivorous grazing, (4) phytoplankton basal metabolism excreted as DOC and POC, (5) DOC and POC excreted by zooplankton basal metabolism or egested during zooplankton feeding, (6) settling of particulate particles, (7) water-sediment DOC exchanges and/or exchanges between epilimnion and hypolimnion, (8) POC dissolution, (9) exogenous inflows of DOC and POC, (10) outflows of DOC and POC to Puget Sound, and (11) DOC sinks due to denitrification and oxic respiration.

solved organic carbon in the water column. [Also note that the fraction of basal metabolism that is exuded as dissolved organic carbon in the model increases as dissolved oxygen concentrations decline (Cerco and Cole, 1994).] A fraction of the particulate organic carbon undergoes first-order dissolution to dissolved organic carbon, while another fraction settles to the sediment. Particulate organic carbon is grazed by zooplankton (detrivory) and organic carbon also enters the system through external loading and is lost with outflows via the Lake Union Ship Canal. Finally, dissolved organic carbon is lost through a first-order denitrification and respiration during heterotrophic activity.

2.4.2. Nitrogen

Four nitrogen state variables are considered by the model: nitrate, ammonium, dissolved and particulate organic nitrogen (see Fig. 4, Part II). Both ammonium and nitrate are incorporated by phytoplankton during growth and Wroblewski's model (1977) was used to describe ammonium inhibition of nitrate uptake. Phytoplankton basal metabolism, zooplankton basal metabolism and egestion of excess nitrogen during zooplankton feeding release ammonium and organic nitrogen in the water column. We used a linear *N*:*P* egestion ratio for zooplankton across the entire range of food *N*:*P*, which is slightly different from Sterner's (1990) curvilinear approach when food *N*:*P* ratios are lower than the grazer's *N*:*P* somatic ratios. A fraction of the particulate organic nitrogen hydrolyzes to dissolved organic nitrogen and another fraction settles to the sediment. Dissolved organic nitrogen is mineralized to ammonium. In an oxygenated water column, ammonium is oxidized to nitrate through nitrification and its kinetics are modeled as a function of available ammonium, dissolved oxygen, temperature and light (Cerco and Cole, 1994; Tian et al., 2001). During anoxic conditions, nitrate is lost as nitrogen gas through denitrification.

2.4.3. Phosphorus

The model considers three phosphorus state variables: phosphate, and dissolved and particulate organic phosphorus (see Fig. 5, Part II). Phytoplankton assimilates phosphate and redistributes the three forms of phosphorus through basal metabolism. Zooplankton basal metabolism and egestion of excess phosphorus during feeding release phosphate and dissolved and particulate organic phosphorus. Particulate organic phosphorus can be hydrolized to dissolved organic phosphorus, and another fraction settles to the sediment. Dissolved organic phosphorus is mineralized to phosphate through a first-order reaction. Particulate organic phosphorus in detritus is grazed by zooplankton. External phosphorus loads to the system and losses via the outflows are also considered.

2.4.4. Silica

Two silica state variables are considered by the model: dissolved available and particulate silica. The silica cycle of the model is very simple and only considers diatom uptake of available dissolved silica, and recycling through basal metabolism in both particulate and dissolved forms. Particulate silica first-order dissolution and settling losses to the sediments are also considered.

2.4.5. Dissolved oxygen

The major sources and sinks of dissolved oxygen in the water column include phytoplankton photosynthesis and respiration, zooplankton and heterotrophic respiration, nitrification and atmospheric reaeration. The rate of the latter process is proportional to the dissolved oxygen deficit, while the dissolved oxygen saturation concentration decreases as temperature and chloride concentrations increase, based on the empirical formula provided by Genet et al. (1974).

2.4.6. Fluxes from the sediment

The model considers sediment–water interactions since these are critical component for predicting the lake's response to different managerial schemes. Significant advances have been made over the past decade for models that simulate the sediment-diagenesis process (e.g., Di Toro et al., 1990; Cerco and Cole, 1994; Penn et al., 1995). However, the existing information for Lake Washington is limited and restrictive for including a dynamic sediment submodel (i.e., without a significant increase in overall model uncertainty). Hence, we followed a simpler dynamic approach that relates sediment oxygen consumption, and nitrogen and phosphorus fluxes with sedimentation and burial rates while also accounting for temperature (e.g., note the absence of model formulations that simulate impacts of hypoxia on redox-sensitive biogeochemical

processes and nutrient cycling). The relative magnitudes of ammonium and nitrate fluxes were determined by nitrification occurring at the sediment surface. This simplified approach is often critisized as being inadequate for representing sediment dynamics and for having limited predictive power (Reckhow and Chapra, 1999). Nonetheless, in this particular case, the parameter values for these relationships were assigned prior to model calibration and were based on estimates from nutrient budget calculations and some field measurements that cover a wide range of nutrient loading in Lake Washington (prediversion period, transient phase and current conditions) (Edmondson and Lehman, 1981; Kuivila and Murray, 1984; Quay et al., 1986; Kuivila et al., 1988; Devol, pers. comm.), which adds validity in approximating sediment response or at least for estimating net total annual sediment fluxes.

3. Sensitivity analysis and discussion

3.1. Screening test

The first set of simulations was designed as a screening tool to identify the most influential model parameters for the environmental variables measured by the Major Lakes Monitoring Program of King County, Washington State, USA (KCWQR, 2000; see also Arhonditsis et al., 2003, for sampling and analytical details). In this initial test, we did not include parameters related to phytoplankton or zooplankton stoichiometry, the temperature-dependence of biochemical processes, zooplankton food preferences and food quality. These parameters will be addressed later in Part II of this study. Each of the parameters used was assigned ranges based on published literature values (see Appendix B for references) and, for the shake of simplicity, the respective spaces were independently sampled as log-normal distributions (e.g., Steinberg et al., 1997) [note, however, that both the shape of the input distributions and the parameter interdependencies (correlations) can play a major role on the sensitivity analysis results]. In order to maintain the functional characteristics that differentiate the phytoplankton and zooplankton groups, we combined the independent sampling for each group with appropriate restrictions (e.g., $\text{growth}_{\max(\text{diat})} > \text{growth}_{\max(\text{greens})} > \text{growth}_{\max(\text{cyan})}$), and sets that did not meet these requirements were excluded. The predefined criteria for considering a model run as acceptable were: (a) positive values for all the state variables, (b) phytoplankton biomass that did not exceed a chlorophyll a concentration of $25\,\mu g\,l^{-1}$ (based on C/chl = 50), (c) total phosphorus concentrations that did not exceed $50\,\mu g\,l^{-1}$ and (d) total nitrogen concentrations that did not exceed $600\,\mu g\,l^{-1}$. These values were chosen to represent the highest observed values in Lake Washington during its recovered state (i.e., from 1975 to present; see Arhonditsis et al., 2003, 2004b). The model was run for 10 annual cycles, which was sufficient time to reach an equilibrium state (i.e., reproduce similar annual cycles) or to collapse (zero, negative values or approach infinity). [Note that here the term "collapse" is not strictly associated with the Liapunov stability notion.] Averaged observed January values for 1995–2001 were used as initial conditions for all state variables. The model forcing functions also represented mean lake patterns, as described in Section 2.1. We generated 10^5 parameter sets and eventually 754 model runs met these criteria and were classified as acceptable.

The five most influential parameters – ranked by their semi-partial coefficients of determination (r^2_{spart}) – from the multiple regression models for phytoplankton and zooplankton biomass, phosphate, total phosphorus, nitrate, total nitrogen, dissolved oxygen, total organic carbon and total silica concentrations and the proportion of cyanobacteria are presented in Table 1. These models are based on mean values for the 10th annual simulation cycle, averaged over the epilimnion and hypolimnion. In all cases, the model r^2-values were high (>0.85) which indicates that within the selected layout (parameter ranges, state variables accepted values) the relationship between the input parameters and model outputs can be approximated as linear and the system does not reach its carrying capacity. Zooplankton maximum grazing rate and phytoplankton basal metabolism have the most significant effects on phytoplankton biomass and together account for about 47% of the overall observed variability. Phytoplankton biomass was also sensitive to the maximum phytoplankton growth rate ($r^2_{\text{spart}} = 0.139$), the zooplankton half saturation constant for grazing ($r^2_{\text{spart}} = 0.117$) and background light attenuation ($r^2_{\text{spart}} = 0.102$). Significant proportion of the zooplankton biomass variability can be explained by the phytoplankton maximum growth rate ($r^2_{\text{spart}} = 0.288$), background light

Table 1
Global sensitivity analysis of the Lake Washington eutrophication model

Phytoplankton (0.951)	r^2_{spart}	Zooplankton (0.958)	r^2_{spart}	Phosphate (0.938)	r^2_{spart}	Total phosphorus (0.901)	r^2_{spart}	Nitrate (0.979)	r^2_{spart}
$grazing_{max(j)}$*	0.262	$growth_{max(i)}$	0.288	$bm_{ref(i)}$	0.259	$bm_{ref(i)}$	0.201	$growth_{max(i)}$*	0.254
$bm_{ref(i)}$*	0.205	$K_{EXTback}$*	0.231	$growth_{max(i)}$*	0.211	$growth_{max(i)}$*	0.198	$grazing_{max(j)}$	0.202
$growth_{max(i)}$	0.139	$bm_{ref(i)}$*	0.151	$K_{EXTback}$	0.190	$K_{EXTback}$	0.165	$K_{EXTback}$	0.191
$KZ_{(j)}$	0.117	$Pred_1$*	0.114	$KP_{(i)}$	0.164	$KP_{(i)}$	0.152	$KZ_{(j)}$*	0.125
$K_{EXTback}$*	0.102	$grazing_{max(j)}$*	0.090	$V_{settling(i)}$	0.068	$grazing_{max(j)}$*	0.093	$bm_{ref(i)}$	0.083

Total nitrogen (0.945)	r^2_{spart}	Dissolved oxygen (0.867)	r^2_{spart}	Total organic carbon (0.911)	r^2_{spart}	Total silica (0.872)	r^2_{spart}	Epilimnetic cyanobacteria (0.930)	r^2_{spart}
$bm_{ref(i)}$	0.227	$Kref_{respdoc}$*	0.298	$Kref_{respdoc}$*	0.351	$growth_{max(i)}$*	0.295	$grazing_{max(j)}$	0.244
$VP_{settling}$*	0.215	$FBM_{DOC(i,j)} - FE_{DOC(j)}$	0.180	$KZ_{(j)}$	0.137	$bm_{ref(j)}$	0.198	$V_{settling(i)}$	0.112
$FBM_{PON(i,j)} - FE_{PON(j)}$*	0.179	$KZ_{(j)}$*	0.078	$grazing_{max(j)}$*	0.131	$grazing_{max(j)}$	0.069	$Pred_1$*	0.093
$KNref_{mineral}$*	0.078	$Pred_1$*	0.073	$Pred_1$	0.099	$VPSi_{settling}$*	0.069	$KZ_{(j)}$*	0.091
$KNref_{dissolution}$	0.056	$VP_{settling}$*	0.065	$VP_{settling}$*	0.070	$Pred_1$*	0.067	$bm_{ref(i)}$*	0.085

Model parameters with the most significant effects on phytoplankton biomass, zooplankton biomass, phosphate, total phosphorus, nitrate, total nitrogen, dissolved oxygen, total organic carbon, total silica and epilimnetic proportion of cyanobacteria. Ranking was based on the values of squared semi-partial coefficients (r^2_{spart}) for the annual averages (averages weighted over the epilimnion and hypolimnion volumes) of the model outputs. The parentheses indicate the r^2 value of the respective multiple regression models ($n = 754$).

* Negative sign of the regression model parameter.

attenuation ($r^2_{spart} = 0.231$) and phytoplankton basal metabolism ($r^2_{spart} = 0.151$). In addition, the zooplankton specific predation rate was another significant parameter that explained about 11.5% of the annual observed variability for zooplankton biomass. Generally, these parameters were also ranked amongst the five most influential for the other state variables, which is an expected result since they are the chemical variables (e.g., phosphate, nitrate) that interact with the biological components of the system. The impact of the dissolved organic carbon respiration rate on dissolved oxygen and total organic carbon outputs explained 29.8 and 35.1% of the observed variability for these state variables, respectively. Moreover, three parameters associated with nitrogen recycling (the fraction of particulate organic nitrogen supplied to the water column during zooplankton feeding or basal metabolism, the nitrogen mineralization and dissolution rates) accounted for 31.3% of the total nitrogen variability. The ecological implications of this result and its relation to the model structure will be discussed in Part II. Finally, we also included the proportion of cyanobacteria in the epilimnion in this analysis. Three out of the five most important parameters were the same as for phytoplankton biomass ($grazing_{max(j)}$, $KZ_{(j)}$, $bm_{ref(i)}$); and the other two parameters were the phytoplankton specific settling velocities ($r^2_{spart} = 0.112$) and the zooplankton specific predation rate ($r^2_{spart} = 0.093$). It should be pointed out, however, that the three zooplankton parameters ($grazing_{max(j)}$, $KZ_{(j)}$, $pred_1$) accounted for 42.8% of the total variance, which suggests the significance of zooplankton preferences parameterization (based on Appendix B values, in these numerical experiments) for modeling shifts in phytoplankton community composition.

3.2. Identifiability analysis

The second set of numerical experiments examined the most influential model parameters with respect to the key state variables for eutrophication models, i.e., phytoplankton and zooplankton biomass, nitrate and phosphate concentrations, and the proportion of cyanobacteria. Parameter selection was based on the coefficient of determination values from the screening test, which decreased quasi-continuously but had clear-cut differences that facilitated the selection of the optimally sized parameter-set. The twenty most

Table 2
Component coefficients for the four principal components extracted from the PCA of the standardized regression coefficients

Parameter	Ecological group	PC1 (42%)	PC2 (25%)	PC3 (13%)	PC4 (8%)
$K_{EXTback}$	Phytoplankton	0.835	−0.331	−0.007	0.218
$K_{EXTchla}$	Phytoplankton	0.901	−0.389	−0.026	−0.016
$V_{settling(i)}$	Phytoplankton	0.356	−0.317	−0.406	0.733
$bm_{ref(i)}$	Phytoplankton	0.736	−0.452	0.034	−0.464
$growth_{max(i)}$	Phytoplankton	−0.934	0.293	−0.075	−0.036
$KP_{(i)}$	Phytoplankton	0.524	−0.645	0.040	−0.439
$bm_{ref(j)}$	Zooplankton	−0.626	−0.675	−0.182	0.201
$grazing_{max(j)}$	Zooplankton	0.808	0.456	−0.166	0.124
$KZ_{(j)}$	Zooplankton	−0.848	−0.426	0.237	−0.095
$pred_1$	Zooplankton	−0.324	−0.415	0.816	0.108
ef_2	Zooplankton	−0.596	−0.777	0.108	0.115
$VP_{settling}$	Various processes	0.097	−0.723	0.375	0.154
$KNref_{dissolution}$	Various processes	−0.158	−0.132	−0.402	−0.477
$KPref_{dissolution}$	Various processes	−0.262	−0.188	−0.495	−0.539
$KNref_{mineral}$	Various processes	−0.201	−0.622	−0.402	−0.002
$KPref_{mineral}$	Various processes	−0.232	−0.667	−0.509	−0.035
$FBM_{PO_4(i,j)} - FE_{PO_4(j)}$	Nutrient recycling	−0.519	−0.319	−0.691	0.049
$FBM_{DOP(i,j)} - FE_{DOP(j)}$	Nutrient recycling	0.058	0.107	0.449	−0.010
$FBM_{NH_4(i,j)} - FE_{NH_4(j)}$	Nutrient recycling	−0.492	−0.302	−0.655	0.012
$FBM_{DON(i,j)} - FE_{DON(j)}$	Nutrient recycling	0.057	0.100	0.383	−0.003

The used state variables were phytoplankton, zooplankton, phosphate and nitrate along with the epilimnetic proportion of cyanobacteria. The column labeled "Ecological group" indicates the group that each parameter was linked according to its ecological role.

influential parameters are reported in Table 2, where they are divided into groups that indicate their ecological roles (Column 2 labeled "Ecological group"). The procedure (sampling method, initial conditions, forcing functions) was the same as for the screening test, while the other parameters were set at fixed values that corresponded to the final model solution (calibration values, see Appendix B and Part II). We used an alternative scheme for the plankton groups based on sampling for the diatoms and cladocerans, and the values for the other groups were assigned as a relative change to their final calibration values. For example, the maximum growth rate in the final model solution was 2.20 day^{-1} for diatoms, 1.80 day^{-1} for greens and 1.20 day^{-1} for cyanobacteria. When a value of 2.30 day^{-1} is sampled for diatoms, the corresponding values for the other two groups were set to 1.88 and 1.25 day^{-1}, respectively. The basic flaw of this approach is that it does not explore the entire parameter space. However, we found that the scheme used in the screening test dramatically decreased the number of acceptable runs due to competitive exclusions between the plankton groups.

We developed multiple regression models ($n = 400$) for monthly averages (of the 10th simulation cycle) for the five environmental variables, and then applied principal component analysis to the resulting 20×60 matrix of the standardised regression coefficients to gain information about the identifiability of the parameters. The four principal components extracted accounted for 88% of the overall variability and the parameter loadings are presented in Table 2. The two parameters associated with light attenuation ($K_{EXTback}$ and $K_{EXTchla}$), phytoplankton basal metabolism ($bm_{(i)}$) and the maximum zooplankton grazing rate ($grazing_{max(j)}$) had the highest positive loadings on the first principal component and phytoplankton maximum growth rate ($growth_{max(i)}$) and zooplankton half saturation constant for grazing ($KZ_{(j)}$) had the highest negative loadings. As previously described, these parameters are closely related to phytoplankton and zooplankton dynamics and have high tuning importance for the model since this principal component explains 42% of the overall variability. The half saturation constant for growth efficiency ($ef_{2(j)}$), the settling velocity for particles ($VP_{settling}$) and zooplankton basal metabolism ($bm_{(j)}$) have the highest loadings for the second component. The third principal component is associated with the specific zooplankton predation rate ($pred_1$) and the fractions of inorganic nutrients (NH_4, PO_4)

egested or excreted by phytoplankton and zooplankton ($FBM_{PO_4,NH_4(i,j)} - FE_{PO_4,NH_4(j)}$). In addition, the mineralization and dissolution rates have moderately high loadings, which suggests this component is also associated with nutrient recycling in the model. Finally, the fourth component is mainly related with the phytoplankton settling velocity ($V_{settling(i)}$), which in the screening test was found to be particularly influential for the proportion of cyanobacteria in the epilimnion. It should be noted that the fourth PC has an eigenvalue >1, but is not significant according to the Rule of N (Overland and Preisendorfer, 1982). Table 2 can also be very useful for understanding parameter identifiability. For example, parameters that have approximately the same loadings on the most important principal components have non-identifiable effects. Characteristic cases are the half saturation constant for phosphorus uptake ($KP_{(i)}$) with the phytoplankton basal metabolism ($bm_{(i)}$), and the two parameters associated with light attenuation in the water column ($K_{EXTback}$ and $K_{EXTchla}$). These parameters are practically non-identifiable if monthly data are collected for phytoplankton and zooplankton biomass, phosphate and nitrate concentrations. Also, non-identifiability exists between parameters that have approximately the same loadings but opposite signs for the most important principal components. This is particularly clear between the maximum phytoplankton growth rate ($growth_{max(i)}$) and the background light attenuation ($K_{EXTback}$) or the phytoplankton basal metabolism ($bm_{(i)}$). This is also true for the maximum grazing rate ($grazing_{max(j)}$) and the zooplankton half saturation constant for grazing ($KZ_{(j)}$). In all of these cases, a small change in one parameter can be balanced by appropriate adjustment to the other (i.e., compensating effects).

The standardized regression coefficients of the five most influential parameters based on the monthly averages for epilimnetic phytoplankton biomass, total zooplankton biomass and the proportion of cyanobacteria are presented in Figs. 3–5. These plots show the variability in the importance of each parameter during the annual cycle, which can also be indicative of the nature of the driving forces that control system dynamics. During the first months of the year, when the system is light-limited, the background light attenuation has its lowest values ($s_b \approx -0.40$) and together with the maximum growth rate ($s_b \approx 0.50$) are the most important parameters for the epilimnetic phytoplankton biomass. [Also, note the opposite signs of the two parameters and the similar compensation that can be provided by phytoplankton basal metabolism.] After initiation of the spring bloom, zooplankton populations progressively respond but do not exert a significant grazing pressure until April as can be inferred by the maximum grazing rate values. The main reason is that low winter water temperatures limit cladoceran growth, however as the epilimnion warms in May (according to the sinusoidal temperature function) an abrupt decrease in this coefficient ($s_b \approx -0.70$) occurs. From this point on, the system is dominated by zooplankton grazing and consequently undergoes prey–predator oscillations. The half saturation for zooplankton grazing progressively increases during late summer–early fall ($s_b \approx 0.40$), showing the importance of the competitive properties of zooplankton grazing at relatively low food concentrations (with non-limiting physical conditions) for phytoplankton dynamics. In addition, the observed summer fluctuations in the maximum growth rate, background light attenuation and phytoplankton basal metabolism, when using zooplankton biomass as dependent variable, are also indicative of a tight phytoplankton–zooplankton relationship (Fig. 4). The negative summer regression coefficients for the maximum grazing rate, especially in June ($s_b \approx -0.80$), show a negative feedback induced by zooplankton when higher parameter values are assigned and the resultant decrease in phytoplankton biomass has a negative impact on zooplankton survivorship. Predation on zooplankton has a local minimum value in May ($s_b \approx -0.40$) and a decreasing trend from July to October (annual minimum $s_b \approx -0.55$), which also influences zooplankton dynamics. Finally, the positive relationship between the maximum grazing rate and the proportion of cyanobacteria in the epilimnion reflects the role of the assigned zooplankton preferences for the four food-types, which seem to promote cyanobacteria in their competition with the other two groups. These preferences are mostly driven by the various food concentrations (especially for cladocerans) and this explains the maximum values in May–June ($s_b \approx 0.50$), when diatoms and greens dominate the system. As also indicated in Section 2.1, higher phytoplankton settling velocities also elicit a competitive advantage for cyanobacteria, especially during the summer stratified period ($s_b \approx 0.40$) when greens and especially diatoms tend to settle out of the water column.

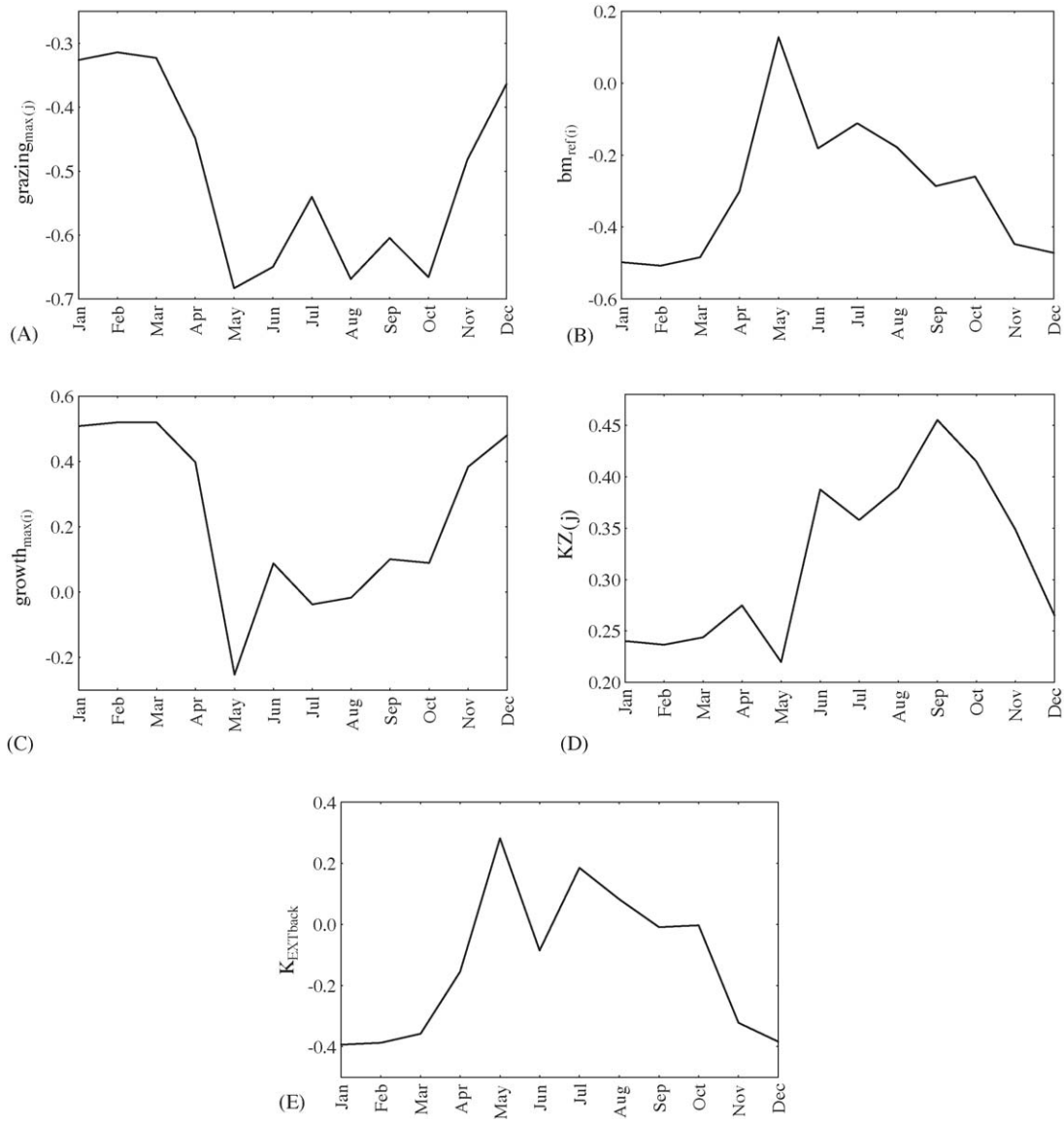

Fig. 3. Annual variability of the maximum grazing rate (A), phytoplankton basal metabolism (B), maximum growth rate (C), half saturation constant for zooplankton feeding (D), background light attenuation (E) standardized regression coefficients for epilimnetic phytoplankton biomass.

3.3. Stoichiometric parameters

During the initial screening test, the parameters related to phytoplankton and zooplankton stoichiometry were fixed at the means for their defined range, and we thus did not consider their contribution to model sensitivity. This actually means that the previously described analysis is based on variable phytoplankton stoichiometry, but it does not take into account the importance of different ranges of nutrient storage (maximum and minimum internal concentrations) and maximum uptake rates on the model outputs and their interactions with the rest of the kinetic parameters. We carried out two numerical experiments to address these issues. We used

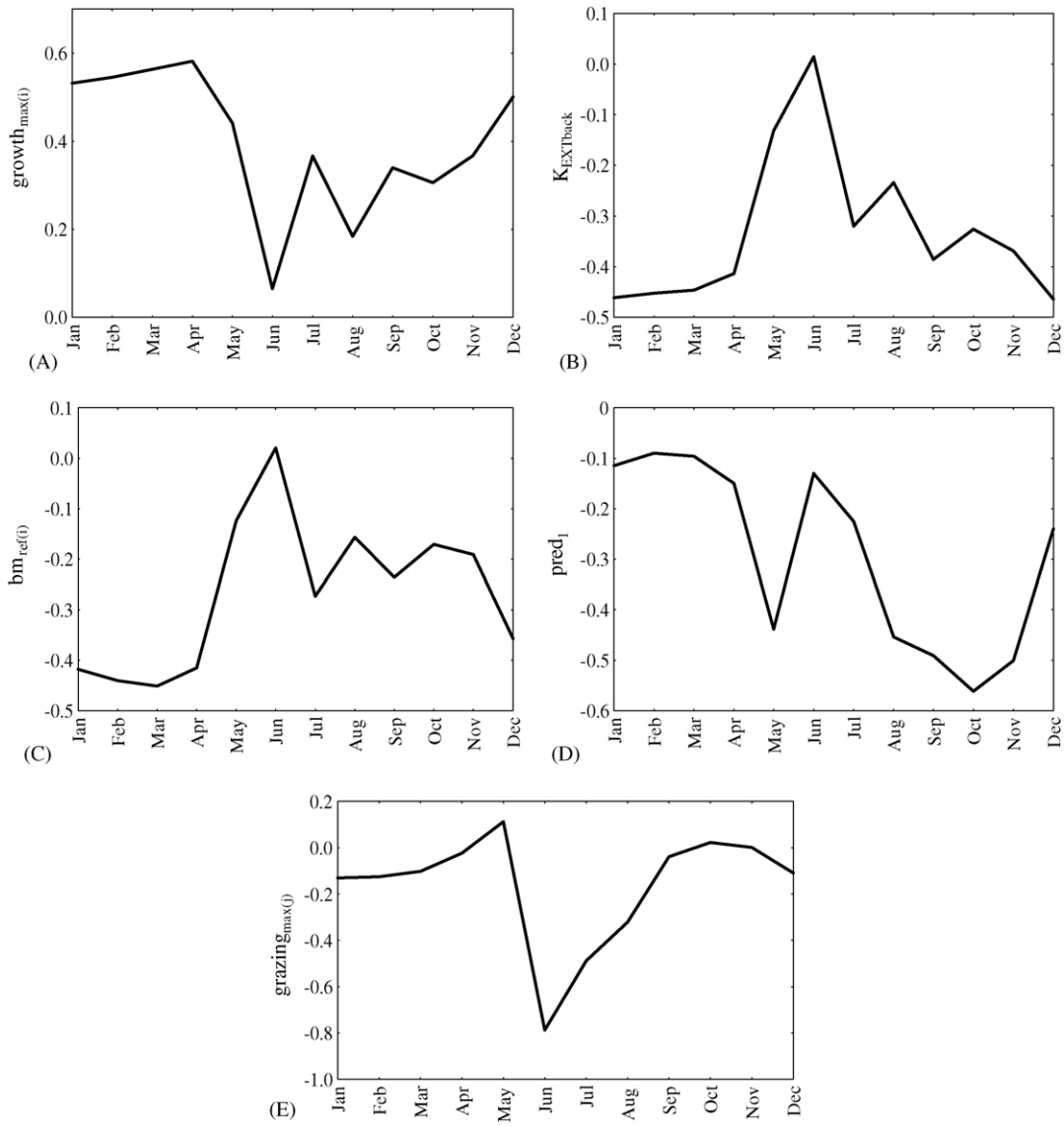

Fig. 4. Annual variability of the maximum growth rate (A), background light attenuation (B), phytoplankton basal metabolism (C), specific zooplankton predation rate (D), maximum grazing rate (E) standardized regression coefficients for zooplankton biomass.

the same sampling scheme from the parameter ranges (log-normal distribution), while the other parameters were fixed at their final calibration values (Appendix B). The three phytoplankton groups had the same stoichiometric parameter values, and so the differences in their internal nutrient content were due to the different growth rates and half saturation constants. On the other hand, the zooplankton stoichiometries were sampled for cladocerans and a relative change according to their *C*:*N* and *C*:*P* calibration ratios was assigned to copepods. We developed multiple regression models for both monthly and annual averages for epilimnetic and hypolimnetic phytoplankton biomass, the proportion of cyanobacteria and total zooplankton biomass.

The first set of numerical experiments evaluated the relative importance of the eight stoichiometric pa-

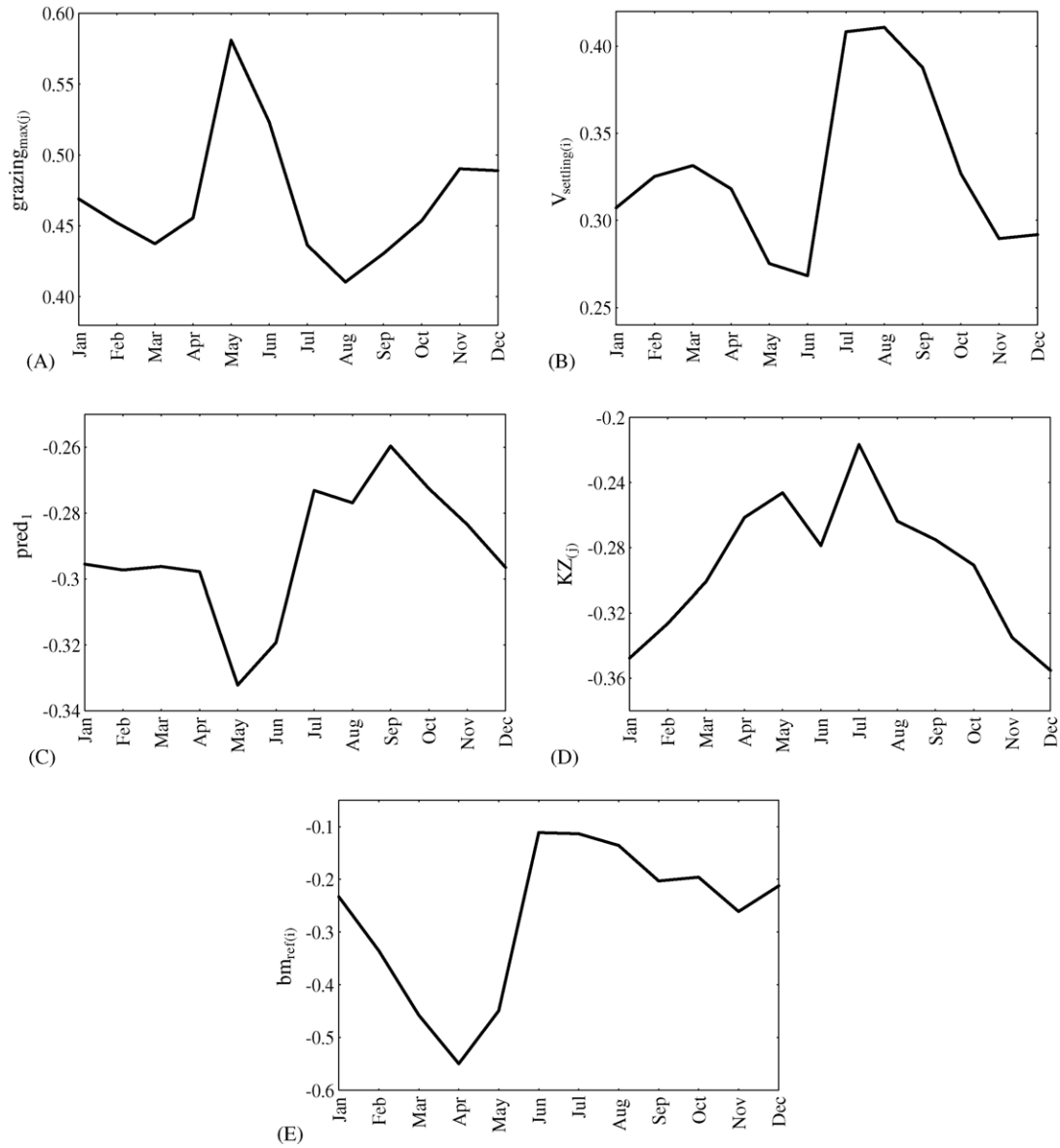

Fig. 5. Annual variability of the maximum grazing rate (A), phytoplankton settling velocity (B), specific zooplankton predation rate (C), half saturation constant for zooplankton feeding (D), phytoplankton basal metabolism (E) standardized regression coefficients for epilimnetic cyanobacteria biomass.

rameters (Table 3). None of the stoichiometric parameters related to nitrogen had significant effects on the four output variables, which is a plausible result since the simulations were based on the current phosphorus-limited conditions in Lake Washington. The minimum phytoplankton phosphorus content was the most significant parameter for the epilimnetic phytoplankton biomass ($r^2_{spart} = 0.513$) as well as total zooplankton biomass ($r^2_{spart} = 0.492$), and almost exclusively accounted for epilimnetic cyanobacteria variability ($r^2_{spart} = 0.619$). On the other hand, the maximum phytoplankton phosphorus content was most

Table 3
Multiple regression analysis ($n = 150$) of the model parameters related with the ecological stoichiometries

Dependent variable	Independent variable	r^2_{spart}
Epilimnetic phytoplankton biomass (0.903)	$N_{upmax(i)}$*	0.000
	$N_{max(i)}$	0.000
	$N_{min(i)}$	0.000
	$P_{upmax(i)}$	0.134
	$P_{max(i)}$*	0.289
	$P_{min(i)}$*	0.513
	$C/N_{(j)}$*	0.000
	$C/P_{(j)}$*	0.042
Hypolimnetic phytoplankton biomass (0.943)	$N_{upmax(i)}$*	0.000
	$N_{max(i)}$	0.000
	$N_{min(i)}$*	0.000
	$P_{upmax(i)}$	0.276
	$P_{max(i)}$*	0.468
	$P_{min(i)}$*	0.279
	$C/N_{(j)}$*	0.000
	$C/P_{(j)}$*	0.026
Proportion of cyanobacteria (0.841)	$N_{upmax(i)}$*	0.006
	$N_{max(i)}$*	0.001
	$N_{min(i)}$	0.001
	$P_{upmax(i)}$*	0.001
	$P_{max(i)}$*	0.088
	$P_{min(i)}$*	0.619
	$C/N_{(j)}$	0.000
	$C/P_{(j)}$*	0.156
Total zooplankton biomass (0.878)	$N_{upmax(i)}$*	0.000
	$N_{max(i)}$*	0.000
	$N_{min(i)}$*	0.000
	$P_{upmax(i)}$	0.152
	$P_{max(i)}$*	0.200
	$P_{min(i)}$*	0.492
	$C/N_{(j)}$*	0.000
	$C/P_{(j)}$*	0.061

The symbol r^2_{spart} corresponds to the squared semi-partial coefficient and the parentheses indicate the r^2 value of the respective multiple regression models (based on the annual averages of the dependent variables).

* Negative sign of the regression model parameter.

influential for hypolimnetic phytoplankton biomass ($r^2_{spart} = 0.468$), had an important role on the epilimnetic phytoplankton biomass ($r^2_{spart} = 0.289$) and total zooplankton biomass ($r^2_{spart} = 0.200$), but only had a minor effect on the proportion of the epilimnetic cyanobacteria ($r^2_{spart} = 0.088$). The maximum phosphorus uptake rate had the greatest on hypolimnetic phytoplankton biomass ($r^2_{spart} = 0.276$) and, interestingly, the zooplankton C:P ratio accounted for a significant portion of the epilimnetic cyanobacteria variability ($r^2_{spart} = 0.156$). We further explored the role of the four phosphorus stoichiometric parameters by plotting the monthly-standardized regression coefficients with the epilimnetic phytoplankton biomass as dependent variable (Fig. 6). An apparent trade-off exists between the roles of the maximum and minimum phytoplankton phosphorus content during the stratified and the non-stratified period. In addition, the maximum phosphorus uptake was lowest during May–June and was closer to the trends for the maximum phosphorus content. A similar relatioship was already described between the annual averages of the epilimnetic and hypolimnetic phytoplankton biomass and should be associated with the ambient phosphorus concentrations. When phosphorus concentrations are high (i.e., well above the half saturation constant) the maximum phosphorus content has a significant role. As nutrient concentrations decrease, phosphorus becomes limiting for the phytoplankton and its role is progressively replaced by the minimum phosphorus content. The monthly-standardized regression coefficients with the hypolimnetic phytoplankton biomass as a dependent variable (not plotted here) agree with this pattern. These results showed the same role exchange, which however occurred over a shorter period (May–August) since hypolimnetic phosphorus accumulation accelerates the dominance of phytoplankton maximum uptake rate and phosphorus content. In addition, during the summer stratified period, epilimnetic cyanobacteria are more responsive to phosphorus stoichiometric changes, since optimal temperature conditions and lower settling velocities reduce their handicap as phosphorus competitors. This explains their strong association primarily with the concurrently significant role of minimum phosphorus content and secondarily with zooplankton C:P ratios (which is additional source of phosphorus through recycling) as shown in Table 3. On the other hand, the other two stoichiometric parameters ($P_{upmax(i)}$, $P_{max(i)}$) have weak relationships, because their "winter" role is eliminated by the other cyanobacteria competitive limitations.

The second set of numerical experiments evaluates the relative importance of and interactions between the four phosphorus stoichiometric parameters and three of the most influential kinetic parameters (maximum phytoplankton growth rate and basal metabolism rates and

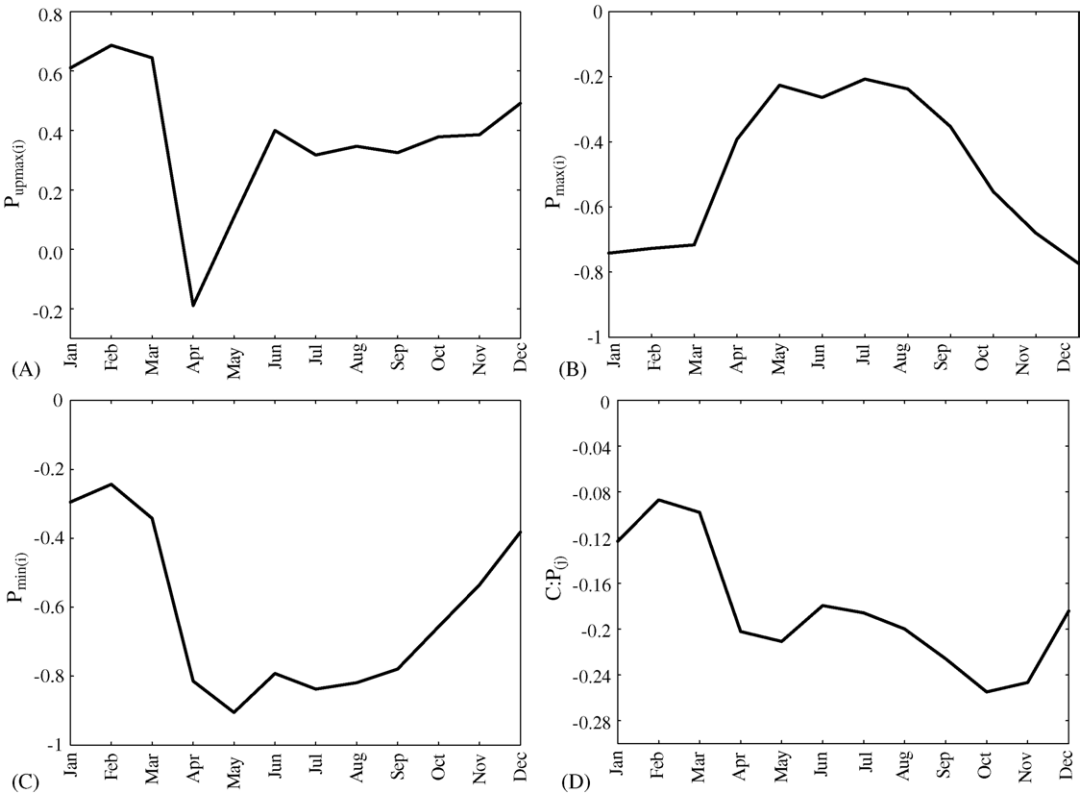

Fig. 6. Annual variability of the standardized regression coefficients of the phytoplankton maximum uptake rate, maximum and minimum phosphorus content (A–C) and zooplankton *C*:*P* ratio (D) for epilimnetic phytoplankton biomass.

maximum zooplankton grazing rate). We also included the half saturation constant for zooplankton growth efficiency, because it is a parameter introduced by the present study and we wanted to look for influences on the remaining model structure (Table 4). Generally, the kinetic parameters dominated over the stoichiometric and explained most of the observed variability, with the exception being the minimum internal phosphorus for the epilimnetic phytoplankton ($r^2_{spart} = 0.158$) and total zooplankton biomass ($r^2_{spart} = 0.256$). Furthermore, the monthly-standardized regression coefficients did not show marked deviations from the reported patterns in Figs. 3–6. Interestingly, an inversion of the maximum growth rate and minimum internal phosphorus impact occurs in April, which stresses the role of phosphorus limitation as another component of the spring phytoplankton dynamics in addition to zooplankton grazing (Fig. 7).

3.4. Forcing functions

The final part of the sensitivity analysis examined the effects of the forcing functions on the model outputs. We assessed the influence of uncertainties in water temperature, solar radiation, external nutrient loading, epilimnion volume, diffusivity values and sediment–water exchanges. Based on the coefficients of variation for interannual variability, these values were 15, 15, 40, 10, 10 and 20% for water temperature, solar radiation, external nutrient loading, epilimnion volume, diffusivity values and sediment–water exchanges, respectively. We only used interannual variability because the perturbations were tested as shifts in the mean annual value for each forcing function and not seasonally or on individual months. For example, as previously mentioned, both solar radiation and epilimnetic and hypolimnetic water temperature were in-

Table 4
Multiple regression analysis ($n = 150$) of the most important model parameters for phytoplankton biomass and phosphorus stoichiometries

Dependent variable	Independent variable	r^2_{spart}
Epilimnetic phytoplankton biomass (0.918)	$growth_{max(i)}$	0.117
	$bm_{ref(i)}$*	0.259
	$grazing_{max(j)}$*	0.386
	$ef_{2(j)}$	0.023
	$P_{upmax(i)}$	0.035
	$P_{max(i)}$*	0.080
	$P_{min(i)}$*	0.158
	$C/P_{(j)}$*	0.014
Hypolimnetic phytoplankton biomass (0.936)	$growth_{max(i)}$	0.177
	$bm_{ref(i)}$*	0.555
	$grazing_{max(j)}$*	0.250
	$ef_{2(j)}$	0.015
	$P_{upmax(i)}$	0.032
	$P_{max(i)}$*	0.048
	$P_{min(i)}$*	0.035
	$C/P_{(j)}$*	0.002
Proportion of cyanobacteria (0.863)	$growth_{max(i)}$*	0.027
	$bm_{ref(i)}$*	0.118
	$grazing_{max(j)}$	0.469
	$ef_{2(j)}$*	0.052
	$P_{upmax(i)}$*	0.000
	$P_{max(i)}$*	0.003
	$P_{min(i)}$*	0.054
	$C/P_{(j)}$*	0.018
Total zooplankton biomass (0.883)	$growth_{max(i)}$	0.248
	$bm_{ref(i)}$*	0.208
	$grazing_{max(j)}$	0.004
	$ef_{2(j)}$*	0.024
	$P_{upmax(i)}$	0.084
	$P_{max(i)}$*	0.116
	$P_{min(i)}$*	0.256
	$C/P_{(j)}$*	0.048

The symbol r^2_{spart} corresponds to the squared semi-partial coefficient, while the parentheses indicate the r^2 value of the respective multiple regression models (based on the annual averages of the dependent variables).
* Negative sign of the regression model parameter.

cluded as sinusoidal functions and herein the induced perturbations did not modulate the amplitude of the functions around their mean values (i.e., a year with a warm spring and a cold autumn and vice versa), but instead were multiplied with the mean values (i.e., warm or cold years). [An alternative analysis based on individual month perturbations will be discussed in Part II.] Finally, the external nutrient loading range was determined for phosphorus, which is the limiting nutrient in Lake Washington.

Table 5
Multiple regression analysis ($n = 150$) of the model forcing functions

Dependent variable	Independent variable	r^2_{spart}
Epilimnetic phytoplankton biomass (0.965)	Water temperature*	0.087
	Solar radiation*	0.000
	Epilimnion volume*	0.133
	Vertical diffusion*	0.001
	Sediment–water exchanges	0.233
	Exogenous loading	0.400
Hypolimnetic phytoplankton biomass (0.821)	Water temperature*	0.140
	Solar radiation*	0.000
	Epilimnion volume*	0.208
	Vertical diffusion	0.011
	Sediment–water exchanges	0.120
	Exogenous loading	0.243
Proportion of cyanobacteria (0.494)	Water temperature	0.100
	Solar radiation	0.000
	Epilimnion volume*	0.007
	Vertical diffusion	0.021
	Sediment–water exchanges	0.105
	Exogenous loading	0.225
Total zooplankton biomass (0.804)	Water temperature	0.304
	Solar radiation*	0.000
	Epilimnion volume*	0.013
	Vertical diffusion	0.001
	Sediment–water exchanges	0.200
	Exogenous loading	0.250

The symbol r^2_{spart} corresponds to the squared semi-partial coefficient, while the parentheses indicate the r^2 value of the respective multiple regression models (based on the annual averages of the dependent variables).
* Negative sign of the regression model parameter.

The multiple regression models for the annual averages of the epilimnetic and hypolimnetic phytoplankton biomass, proportion of cyanobacteria and total zooplankton biomass are presented in Table 5. In all the cases, the external loading effects were significant as were sediment–water exchanges. Both were positively correlated with the four variables and the same consistent trends were observed with their monthly-standardized regression coefficients (not reported here), and the coefficients of determination accounted for 12–45% of the model output variability. The temperature effects reflect how the model responds to the respective perturbations through the parameters

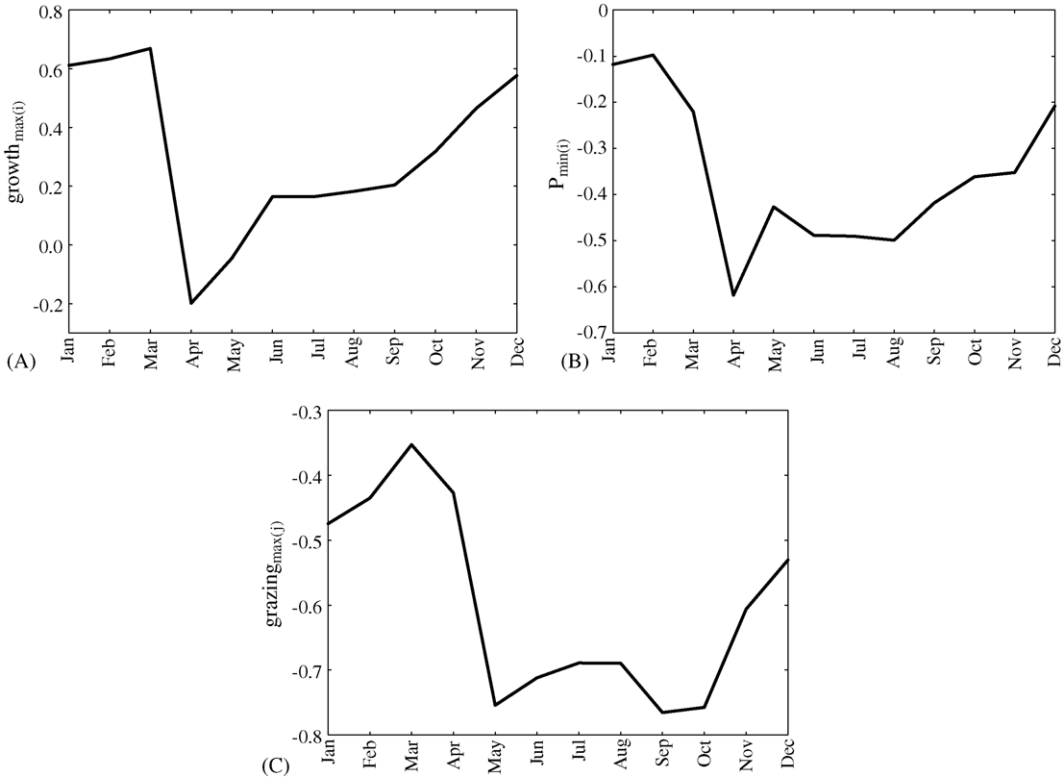

Fig. 7. Annual variability of the maximum growth rate (A), minimum phosphorus content (B) and maximum grazing rate (C) standardized regression coefficients for epilimnetic phytoplankton biomass.

related to temperature-dependence of biochemical processes. These parameters were set at fixed values for the model sensitivity analysis and calibration. It can be seen that temperature is negatively correlated and has a moderately significant impact on epilimnetic ($r^2_{\text{spart}} = 0.087$) and hypolimnetic ($r^2_{\text{spart}} = 0.140$) phytoplankton biomass. Positive correlation and significant influence ($r^2_{\text{spart}} = 0.304$) was found between temperature and total zooplankton biomass, which in turn can in part explain the negative correlation with phytoplankton. Additional support for control of the temperature-phytoplankton relationship due to prey–predator interactions is provided by the low value of the epilimnetic phytoplankton standardized regression coefficient in May ($s_b = -0.628$), and the zooplankton highs in April–May ($s_b \approx 0.600$) (Fig. 8). Similar patterns are observed from October to December and suggest temperature regulates phytoplankton–zooplankton interactions until the lake reaches its winter state. The negative late summer–early fall values for phytoplankton, when zooplankton is nearly unrelated with temperature, indicate the predominance of the basal metabolism losses over the minimal growth of the strongly phosphorus-limited phytoplankton. Interestingly, the annual proportion of cyanobacteria is positively correlated with temperature, especially during the colder months of the year when all the monthly-standardized regression coefficients were positive (0.450–0.850). This is indicative of the relatively stronger temperature limitations assigned to this phytoplankton group (Appendix B). Epilimnion volume has significant effects and a negative relationship with annual epilimnetic phytoplankton biomass ($r^2_{\text{spart}} = 0.133$), especially during the spring bloom ($s_b \geq -0.470$), which indicates the sensitivity of the model in the prescribed two spatial compartments for reproducing phytoplankton dynamics. This is particularly important because if the spatial structure is included in the iterative calibration procedure

we might end up obtaining a "good" fit with the wrong chemical/biological dynamics. Finally, the effects of the diffusivity values were not significant for the annual averages for the four variables, but have an interesting intra-annual variability as shown in Fig. 8E. Positive standardized regression coefficients during the stratified period indicate the stimulating effects of nutrient intrusions from the hypolimnion due to increased diffusivity values. The negative values during the non-stratified period are an artifact of the spatial structure of the model that specifies a maximum epilimnion depth of 20 m during the winter and allows for ver-

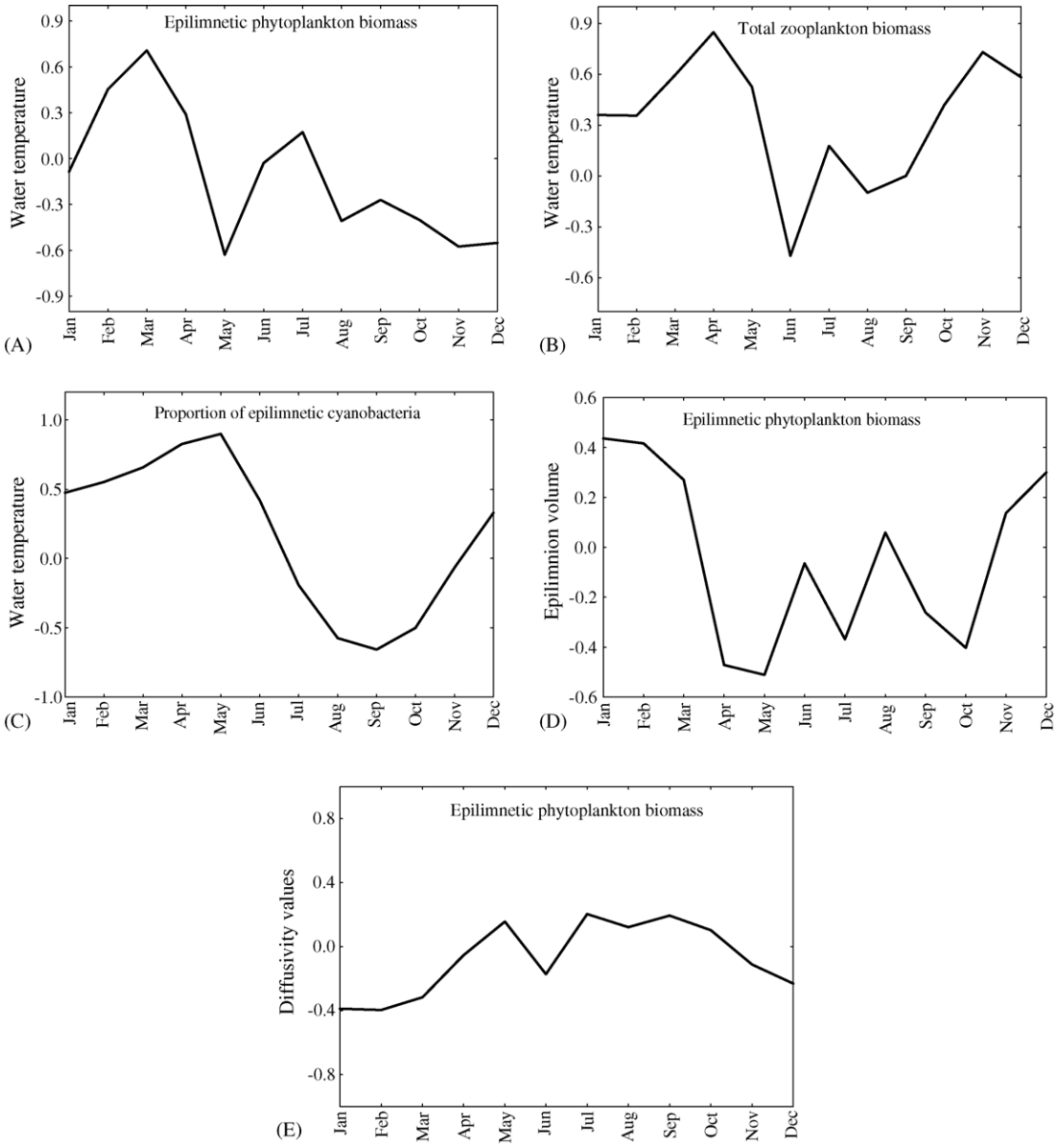

Fig. 8. Annual variability of the water temperature standardized regression coefficients for epilimnetic phytoplankton biomass (A), total zooplankton biomass (B) and proportion of epilimnetic cyanobacteria (C), and the epilimnion volume (D) and vertical diffusion (E) standardized regression coefficients for epilimnetic phytoplankton biomass.

tical phytoplankton gradients and exchanges with the hypolimnion.

4. Conclusions

We described a multi-elemental water quality model developed to address eutrophication scenarios in Lake Washington, USA. The food–web structure of the model makes it possible to relate alternative managerial scenarios and associated nutrient loadings with compositional shifts in the plankton community. The stoichiometrically explicit character of the model also provides a platform for testing recent conceptual advances in nutrient recycling and the extent to which their predictions are observed in the real world. Several parameters associated with plankton kinetics have special tuning importance, and their interrelated impact (i.e., trade-offs, compensating effects) on the model outputs were explored through several numerical experiments. The seasonal role of the explicitly defined epilimnion volume and diffusivity values, suggests the importance of using a hydrodynamic model with a multi-layer vertical system characterization. This will enable a more realistic reproduction of the complex interplay between hydrodynamic, chemical, and food–web interactions, especially during the initiation of the spring bloom and the onset of summer stratification. These results will be used in Part II, where we apply the model to Lake Washington; through a detailed exploration of the nutrient biogeochemical cycles, we suggest issues that should be considered under increased nutrient loading conditions.

Appendix A. Model equations

A.1. Phytoplankton

$$\frac{\partial \mathrm{PHYT}_{(i,x)}}{\partial t} = \mathrm{growth}_{\max(i)} \times f_{\mathrm{nutrient}(i,x)} \times f_{\mathrm{light}(i,x)} \times f_{\mathrm{temperature}(i,x)} \times \mathrm{PHYT}_{(i,x)} - \mathrm{bm}_{\mathrm{ref}(i)}\, \mathrm{e}^{\mathrm{ktbm}(i)(T(x)-\mathrm{Tref}(i))} \times \mathrm{PHYT}_{(i,x)} - V_{\mathrm{settling}(i)} \times f_{\mathrm{temperature}(x)} \times \mathrm{PHYT}_{(i,x)} \times f_{\mathrm{depth}(x)} - \sum_{j=\mathrm{cop,clad}} \mathrm{Grazing}_{(i,j,x)} \times f_{\mathrm{temperature}(j,x)} \times \mathrm{ZOOP}_{(j,x)} - \mathrm{outflows} \times \mathrm{PHYT}_{(i,\mathrm{EPI})} \pm \mathrm{EPI/YPO}_{\mathrm{PHYT}(i)}$$

$$f_{\mathrm{depth(epi)}} = \frac{\text{epilimnion/hypolimnion interface} + \text{epilimnion sediment surface}}{\text{epilimnion volume}}$$

$$f_{\mathrm{depth(hypo)}} = \frac{-\text{epilimnion/hypolimnion interface} + \text{hypolimnion sediment surface}}{\text{hypolimnion volume}}$$

A.1.1. Phytoplankton growth limiting functions

$$f_{\mathrm{nutrient}\,(i,x)} = \min\left\{\frac{N_{(i,x)} - N_{\min(i)}}{N_{\max(i)} - N_{\min(i)}}, \frac{P_{(i,x)} - P_{\min(i)}}{P_{\max(i)} - P_{\min(i)}}\right\}$$

$$f_{\mathrm{light}(i,x)} = \frac{2.718 \times \mathrm{FD}}{K_{\mathrm{EXT}(i,x)} \times \mathrm{depth}_{(x)}} \times (\exp(a) - \exp(b))$$

$$a = -\frac{I_{\mathrm{d}t}}{\mathrm{FD} \times I_{\mathrm{opt}(i,x)}} \times \exp(-K_{\mathrm{EXT}(i,x)} \times (\mathrm{DZ} + \mathrm{depth}_{(x)})), \qquad b = -\frac{I_{\mathrm{d}t}}{\mathrm{FD} \times I_{\mathrm{opt}(i,x)}} \times \exp(-K_{\mathrm{EXT}(i,x)} \times \mathrm{DZ})$$

$T_{(x)}$ is the epilimnion/hypolimnion temperature (°C); $\text{depth}_{(x)}$ the epilimnion/hypolimnion depth (m); I_{dt} the daily illumination at water surface and model day t (Langleys day^{-1}), FD the fractional daylength ($0 \leq \text{FD} \leq 1$), and ZD the distance from water surface to top of model segment (m)

$$I_{\text{opt}(i,x)} = I_{\text{optavg}} \times \exp(-K_{\text{EXT}(i,x)} D_{\text{opt}(i)}), \qquad I_{\text{optavg}} = 0.7 \times I_{dt} + 0.2 \times I_{dt-1} + 0.1 \times I_{dt-2}$$

$$K_{\text{EXT}(i,x)} = I_{o(i)} \times K_{\text{EXT}(x)}, \qquad K_{\text{EXT}(x)} = K_{\text{EXTback}} + K_{\text{EXTchla}} \times \sum_{i=\text{diat, green,cyan}} \frac{\text{PHYT}_{(i,x)}}{C/\text{chl}_{(i)}}$$

$$f_{\text{temperature}(i,x)} = \begin{cases} \exp(-\text{KTgr1}_{(i)}(T_{(x)} - \text{Topt}_{(i)})^2) & \text{when } T_{(x)} \leq \text{Topt}_{(i)} \\ \exp(-\text{KTgr2}_{(i)}(\text{Topt}_{(i)} - T_{(x)})^2) & \text{when } T_{(x)} > \text{Topt}_{(i)} \end{cases}$$

$$f_{\text{temperature}(x)} = \begin{cases} \exp(-\text{KT1}(T_{(x)} - \text{Tref})^2) & \text{when } T_{(x)} \leq \text{Tref} \\ \exp(-\text{KT2}(\text{Tref} - T_{(x)})^2) & \text{when } T_{(x)} > \text{Tref} \end{cases}$$

A.1.2. Phytoplankton stoichiometries

$$\frac{\partial N_{(i,x)}}{\partial t} = N_{\text{up}(i,x)} \times N_{\text{fb}(i,x)} - \text{growth}_{(i,x)} N_{(i,x)}, \qquad \frac{\partial P_{(i,x)}}{\partial t} = P_{\text{up}(i,x)} \times P_{\text{fb}(i,x)} - \text{growth}_{(i,x)} P_{(i,x)}$$

$$\text{growth}_{(i,x)} = \text{growth}_{\max(i)} \times f_{\text{nutrient}(i,x)} \times f_{\text{light}(i,x)} \times f_{\text{temperature}(i,x)}$$

$$N_{\text{up}(i,x)} = N_{\text{up max}(i)} \frac{\text{IN}_{(x)}}{\text{IN}_{(x)} + \text{KN}_{(i)}}, \qquad P_{\text{up}(i,x)} = P_{\text{up max}(i)} \frac{\text{PO4}_{(x)}}{\text{PO4}_{(x)} + KP_{(i)}}$$

$$N_{\text{fb}(i,x)} = \frac{N_{\max(i)} - N_{(i,x)}}{N_{\max(i)} - N_{\min(i)}}, \qquad P_{\text{fb}(i,x)} = \frac{P_{\max(i)} - P_{(i,x)}}{P_{\max(i)} - P_{\min(i)}}$$

A.2. Zooplankton

$$\frac{\partial \text{ZOOP}_{(j,x)}}{\partial t} = \text{gref}_{(j,x)} \times f_{\text{temperature}(j,x)} \times \left(\sum_{i=\text{diat,green,cyan}} \text{Grazing}_{(i,j,x)} + \text{Grazing}_{\text{detritus}(j,x)} \right) \times \text{ZOOP}_{(j,x)} - \text{bm}_{\text{ref}(j)} \text{e}^{\text{ktbm}(j)(T(x) - \text{Tref}(j))} \times \text{ZOOP}_{(j,x)} - \text{predation}_{(j,x)} - \text{outflows} \times \text{ZOOP}_{(j,\text{EPI})}$$

$$f_{\text{temperature}(j,x)} = \begin{cases} \exp(-\text{KTgr1}_{(j)}(T_{(x)} - \text{Topt}_{(j)})^2) & \text{when } T_{(x)} \leq \text{Topt}_{(j)} \\ \exp(-\text{KTgr2}_{(j)}(\text{Topt}_{(j)} - T_{(x)})^2) & \text{when } T_{(x)} > \text{Topt}_{(j)} \end{cases}$$

$$\text{Grazing}_{(i,j,x)} = \frac{\text{grazing}_{\max(j)} \times \text{pref}_{(i,j,x)} \times \text{PHYT}_{(i,x)}}{\text{KZ}_{(j)} + F_{(j,x)}}, \qquad \text{Grazing}_{\text{detritus}(j,x)} = \frac{\text{grazing}_{\max(j)} \times \text{pref}_{\text{det}(j,x)} \times \text{POC}_{(x)}}{\text{KZ}_{(j)} + F_{(j,x)}}$$

$$\text{predation}_{(\text{cop},x)} = \frac{\text{pred}_1 \times \text{ZOOP}^2_{(\text{cop},x)}}{\text{pred}_2 + \text{ZOOP}_{(\text{cop},x)}}, \qquad \text{predation}_{(\text{clad},x)} = \frac{\text{pred}_1 \times \text{ZOOP}^3_{(\text{clad},x)}}{\text{pred}_2^2 + \text{ZOOP}^2_{(\text{clad},x)}}$$

$$F_{(j,x)} = \sum_{i=\text{diat,green,cyan}} \text{pref}_{(i,j,x)} \times \text{PHYT}_{(i,x)} + \text{pref}_{\text{det}(j,x)} \times \text{POC}_{(x)}$$

$$\text{pref}_{(i,j,x)} = \frac{\text{pref}_{(i,j)} \times \text{PHYT}_{(i,x)}}{\sum_{i=\text{diat,green,cyan}} \text{pref}_{(i,j)} \times \text{PHYT}_{(i,x)} + \text{pref}_{\text{det}(j)} \times \text{POC}_{(x)}}$$

$$\text{pref}_{\text{det}(j,x)} = \frac{\text{pref}_{\text{det}(j)} \times \text{POC}_{(x)}}{\sum_{i=\text{diat,green,cyan}} \text{pref}_{(i,j)} \times \text{PHYT}_{(i,x)} + \text{pref}_{\text{det}(j)} \times \text{POC}_{(x)}}$$

$$\text{gref}_{(j,x)} = \frac{\text{ef}_{1(j)} \times \text{FQ}_{(j,x)}}{\text{ef}_{2(j)} + \text{FQ}_{(j,x)}}, \quad \text{FQ}_{(j,x)} = \left(\sum_{i=\text{diat,green,cyan}} \text{FQ}_{(i,j)} \cdot \sqrt{\text{PHYT}_{(i,x)}} + \text{FQ}_{\text{det}(j)} \cdot \sqrt{\text{POC}_{(x)}} \right) \times C/P_{\text{LIM}(j,x)}$$

$$C/P_{\text{LIM}(j,x)} = \begin{cases} \dfrac{\text{GrazC}_{(j,x)}}{\text{GrazP}_{(j,x)}} \leq C:P_0 & 1 \\ \dfrac{\text{GrazC}_{(j,x)}}{\text{GrazP}_{(j,x)}} > C:P_0 & \dfrac{C:P_0}{\text{GrazC}_{(j,x)}/\text{GrazP}_{(j,x)}} \end{cases}$$

$$\frac{\text{GrazC}_{(j,x)}}{\text{GrazP}_{(j,x)}} = \frac{\left(\sum_{i=\text{diat,green,cyan}} \text{Grazing}_{(i,j,x)} + \text{Grazing}_{\text{detritus}(j,x)} \right)}{\left(\sum_{i=\text{diat,green,cyan}} \text{Grazing}_{(i,j,x)} \times P_{(i,x)} + \text{Grazing}_{\text{detritus}(j,x)} \times \text{POP}_{(x)}/\text{POC}_{(x)}{}^{*} \right)}$$

* For copepods, if $\dfrac{\text{POC}_{(x)}}{\text{POP}_{(x)}} > C{:}P_0$, then $1/C{:}P_0$.

A.3. Nitrogen

A.3.1. Nitrate

$$\frac{\partial \text{NO}_{3(x)}}{\partial t} = -\sum_{i=\text{diat,green,cyan}} (1 - \text{prefNH}_{4(i,x)}) \times N_{\text{up}(i,x)} \times N_{\text{fb}(i,x)} \times \text{PHYT}_{(i,x)} + \text{nitrification}_{(x)} - \text{denitrification}_{(x)} - \text{outflows} \times \text{NO}_{3(\text{EPI})} \pm \text{EPI/YPO}_{\text{NO}_3} + \text{NO}_{3\text{EXOG(EPI)}} + \text{NO}_{3\text{ENDOG}(x)}$$

$$\text{prefNH}_4 = 1 - \exp(-\psi_{(i)} \times \text{NH}_{4(x)})$$

$$\text{nitrification}_{(x)} = \text{nitrif}_{\max} \times f_{\text{lightnitr}(x)} \times \frac{\text{DO}_{(x)}}{\text{KH}_{\text{ONIT}} + \text{DO}_{(x)}} \times \frac{\text{NH}_{4(x)}}{\text{KH}_{\text{NH}_4\text{NIT}} + \text{NH}_{4(x)}} \times f_{\text{tempnitr}(x)}$$

$$f_{\text{tempnitr}(x)} = \begin{cases} \exp(-\text{KT}_{\text{nitr1}}(T_{(x)} - \text{Toptnitr})^2) & \text{when } T_{(x)} \leq \text{Toptnitr} \\ \exp(-\text{KT}_{\text{nitr2}}(\text{Toptnitr} - T_{(x)})^2) & \text{when } T_{(x)} > \text{Toptnitr} \end{cases}$$

$$f_{\text{lightnitr}(x)} = \begin{cases} 1 & \text{when } I_{(x)} \leq 0.1 \times I_{\text{d}t} \\ 0 & \text{when } I_{(x)} > 0.1 \times I_{\text{d}t} \end{cases}$$

$$\text{denitrification}_{(x)} = R_{\text{denitr/oxresp}} \times \frac{\text{KH}_{\text{OOXRESP}}}{\text{KH}_{\text{OOXRESP}} + \text{DO}_{(x)}} \times \frac{\text{NO}_{3(x)}}{\text{KH}_{\text{NO}_3\text{DENIT}} + \text{NO}_{3(x)}} \times K_{\text{respdoc}(x)} \times \text{DENIT}_{\text{NO}_3/\text{DOC}} \times \text{DOC}_{(x)}$$

$$K_{\text{respdoc}(x)} = K_{\text{ref}_{\text{respdoc}}} \times f_{\text{temperature}(x)}$$

A.3.2. Ammonium

$$\begin{aligned} \frac{\partial \text{NH}_{4(x)}}{\partial t} = & - \sum_{i=\text{diat,green,cyan}} \text{prefNH}_{4(i,x)} \times N_{\text{up}(i,x)} \times N_{\text{fb}(i,x)} \times \text{PHYT}_{(i,x)} - \text{nitrification}_{(x)} \\ & + \sum_{i=\text{diat,green,cyan}} \text{FBM}_{\text{NH}_4(i)} \times N_{(i,x)} \times \text{bm}_{\text{ref}(i)} \text{e}^{\text{ktbm}(i)(T(x)-\text{Tref}(i))} \times \text{PHYT}_{(i,x)} \\ & + \sum_{j=\text{cop,clad}} \text{FBM}_{\text{NH}_4(j)} \times N/C_{(j)} \times \text{bm}_{\text{ref}(j)} \text{e}^{\text{ktbm}(j)(T(x)-\text{Tref}(j))} \times \text{ZOOP}_{(j,x)} + \text{KN}_{\text{mineral}(x)} \times \text{DON}_{(x)} \\ & + \sum_{j=\text{cop,clad}} \text{FE}_{\text{NH}_4(j)} \times \text{Negestion}_{(j,x)} - \text{outflows} \times \text{NH}_{4(\text{EPI})} \pm \text{EPI/YPO}_{\text{NH}_4} + \text{NH}_{4\text{EXOG}(\text{EPI})} \\ & + \text{NH}_{4\text{ENDOG}(x)} \end{aligned}$$

$$\text{KN}_{\text{mineral}(x)} = \text{KN}_{\text{ref}_{\text{mineral}}} \times f_{\text{temperature}(x)}$$

A.3.3. Dissolved organic nitrogen

$$\begin{aligned} \frac{\partial \text{DON}_{(x)}}{\partial t} = & \sum_{i=\text{diat,green,cyan}} \text{FBM}_{\text{DON}(i)} \times N_{(i,x)} \times \text{bm}_{\text{ref}(i)} \text{e}^{\text{ktbm}(i)(T(x)-\text{Tref}(i))} \times \text{PHYT}_{(i,x)} \\ & + \sum_{j=\text{cop,clad}} \text{FBM}_{\text{DON}(j)} \times N/C_{(j)} \times \text{bm}_{\text{ref}(j)} \text{e}^{\text{ktbm}(j)(T(x)-\text{Tref}(j))} \times \text{ZOOP}_{(j,x)} + \text{KN}_{\text{dissolution}(x)} \\ & \times \text{PON}_{(x)} - \text{KN}_{\text{mineral}(x)} \times \text{DON}_{(x)} + \sum_{j=\text{cop,clad}} \text{FE}_{\text{DON}(j)} \times \text{Negestion}_{(j,x)} - \text{outflows} \times \text{DON}_{(\text{EPI})} \\ & \pm \text{EPI/YPO}_{\text{DON}} + \text{DON}_{\text{EXOG}(\text{EPI})} + \text{DON}_{\text{ENDOG}(x)} \end{aligned}$$

$$\text{KN}_{\text{dissolution}(x)} = \text{KN}_{\text{ref}_{\text{dissolution}}} \times f_{\text{temperature}(x)}$$

A.3.4. Particulate organic nitrogen

$$\frac{\partial \mathrm{PON}_{(x)}}{\partial t} = \sum_{i=\mathrm{diat,green,cyan}} \mathrm{FBM}_{\mathrm{PON}(i)} \times N_{(i,x)} \times \mathrm{bm}_{\mathrm{ref}(i)} \mathrm{e}^{\mathrm{ktbm}(i)(T(x)-\mathrm{Tref}(i))} \times \mathrm{PHYT}_{(i,x)}$$
$$+ \sum_{j=\mathrm{cop,clad}} \mathrm{FBM}_{\mathrm{PON}(j)} \times N/C_{(j)} \times \mathrm{bm}_{\mathrm{ref}(j)} \mathrm{e}^{\mathrm{ktbm}(j)(T(x)-\mathrm{Tref}(j))} \times \mathrm{ZOOP}_{(j,x)}$$
$$- \mathrm{KN}_{\mathrm{dissolution}(x)} \times \mathrm{PON}_{(x)}$$
$$- \sum_{j=\mathrm{cop,clad}} \mathrm{Grazing}_{\mathrm{detritus}(j,x)} \times \mathrm{PON}_{(x)}/\mathrm{POC}_{(x)}(N/C_{(\mathrm{cop})})$$
$$\times f_{\mathrm{temperature}(j,x)} \times \mathrm{ZOOP}_{(j,x)} - \mathrm{VP}_{\mathrm{settling}} \times f_{\mathrm{temperature}(x)} \times \mathrm{PON}_{(x)} \times f_{\mathrm{depth}(x)}$$
$$+ \sum_{j=\mathrm{cop,clad}} \mathrm{FE}_{\mathrm{PON}(j)} \times \mathrm{Negestion}_{(j,x)} - \mathrm{outflows} \times \mathrm{PON}_{(\mathrm{EPI})} + \mathrm{PON}_{\mathrm{EXOG(EPI)}}$$

$$\mathrm{Negestion}_{(j,x)} = \left[\left(\sum_{i=\mathrm{diat,green,cyan}} \mathrm{Grazing}_{(i,j,x)} \times N_{(i,x)} + \mathrm{Grazing}_{\mathrm{detritus}(j,x)} \times \mathrm{PON}_{(x)}/\mathrm{POC}_{(x)}(N/C_{(\mathrm{cop})}) \right) \right.$$
$$\left. - N/P_{(j)} \times \mathrm{gref}_{(j,x)} \times \left(\sum_{i=\mathrm{diat,green,cyan}} \mathrm{Grazing}_{(i,j,x)} \times P_{(i,x)} + \mathrm{Grazing}_{\mathrm{detritus}(j,x)} \times \mathrm{POP}_{(x)}/\mathrm{POC}_{(x)}{}^{*} \right) \right]$$
$$\times f_{\mathrm{temperature}(j,x)} \times \mathrm{ZOOP}_{(j,x)}$$
$$^{*}\text{For copepods if } \frac{\mathrm{POC}_{(x)}}{\mathrm{POP}_{(x)}} > C : P_0 \text{ then } 1/C : P_0$$

A.4. Phosphorus

A.4.1. Phosphate

$$\frac{\partial \mathrm{PO4}_{(x)}}{\partial t} = - \sum_{i=\mathrm{diat,green,cyan}} P_{\mathrm{up}(i,x)} \times P_{\mathrm{fb}(i,x)} \times \mathrm{PHYT}_{(i,x)}$$
$$+ \sum_{i=\mathrm{diat,green,cyan}} \mathrm{FBM}_{\mathrm{PO4}(i)} \times P_{(i,x)} \times \mathrm{bm}_{\mathrm{ref}(i)} \mathrm{e}^{\mathrm{ktbm}(i)(T(x)-\mathrm{Tref}(i))} \times \mathrm{PHYT}_{(i,x)}$$
$$+ \sum_{j=\mathrm{cop,clad}} \mathrm{FBM}_{\mathrm{PO4}(j)} \times P/C_{(j)} \times \mathrm{bm}_{\mathrm{ref}(j)} \mathrm{e}^{\mathrm{ktbm}(j)(T(x)-\mathrm{Tref}(j))} \times \mathrm{ZOOP}_{(j,x)} + \mathrm{KP}_{\mathrm{mineral}(x)} \times \mathrm{DOP}_{(x)}$$
$$+ \sum_{j=\mathrm{cop,clad}} \mathrm{FE}_{\mathrm{PO4}(j)} \times \mathrm{Pegestion}_{(j,x)} - \mathrm{outflows}$$
$$\times \mathrm{PO}_{4(\mathrm{EPI})} \pm \mathrm{EPI/YPO}_{\mathrm{PO4}} + \mathrm{PO}_{4\mathrm{EXOG(EPI)}} + \mathrm{PO}_{4\mathrm{ENDOG}(x)}$$

$$\mathrm{KP}_{\mathrm{mineral}(x)} = \mathrm{KP}_{\mathrm{ref}_{\mathrm{mineral}}} \times f_{\mathrm{temperature}(x)}$$

A.4.2. Dissolved organic phosphorus

$$\frac{\partial \mathrm{DOP}_{(x)}}{\partial t} = \sum_{i=\mathrm{diat,green,cyan}} \mathrm{FBM}_{\mathrm{DOP}(i)} \times P_{(i,x)} \times \mathrm{bm}_{\mathrm{ref}(i)} \mathrm{e}^{\mathrm{ktbm}(i)(T(x)-\mathrm{Tref}(i))} \times \mathrm{PHYT}_{(i,x)}$$
$$+ \sum_{j=\mathrm{cop,clad}} \mathrm{FBM}_{\mathrm{DOP}(j)} \times P/C_{(j)} \times \mathrm{bm}_{\mathrm{ref}(j)} \mathrm{e}^{\mathrm{ktbm}(j)(T(x)-\mathrm{Tref}(j))} \times \mathrm{ZOOP}_{(j,x)} + \mathrm{KP}_{\mathrm{dissolution}(x)}$$
$$\times \mathrm{POP}_{(x)} - \mathrm{KP}_{\mathrm{mineral}(x)} \times \mathrm{DOP}_{(x)} + \sum_{j=\mathrm{cop,clad}} \mathrm{FE}_{\mathrm{DOP}(j)} \times \mathrm{Pegestion}_{(j,x)} - \mathrm{outflows} \times \mathrm{DOP}_{(\mathrm{EPI})}$$
$$\pm \mathrm{EPI}/\mathrm{YPO}_{\mathrm{DOP}} + \mathrm{DOP}_{\mathrm{EXOG(EPI)}} + \mathrm{DOP}_{\mathrm{ENDOG}(x)}$$

$$\mathrm{KP}_{\mathrm{dissolution}(x)} = \mathrm{KP}_{\mathrm{ref}_{\mathrm{dissolution}}} \times f_{\mathrm{temperature}(x)}$$

A.4.3. Particulate organic phosphorus

$$\frac{\partial \mathrm{POP}_{(x)}}{\partial t} = \sum_{i=\mathrm{diat,green,cyan}} \mathrm{FBM}_{\mathrm{POP}(i)} \times P_{(i,x)} \times \mathrm{bm}_{\mathrm{ref}(i)} \mathrm{e}^{\mathrm{ktbm}(i)(T(x)-\mathrm{Tref}(i))} \times \mathrm{PHYT}_{(i,x)}$$
$$+ \sum_{j=\mathrm{cop,clad}} \mathrm{FBM}_{\mathrm{POP}(j)} \times P/C_{(j)} \times \mathrm{bm}_{\mathrm{ref}(j)} \mathrm{e}^{\mathrm{ktbm}(j)(T(x)-\mathrm{Tref}(j))} \times \mathrm{ZOOP}_{(j,x)} - \mathrm{KP}_{\mathrm{dissolution}(x)} \times \mathrm{POP}_{(x)}$$
$$- \sum_{j=\mathrm{cop,clad}} \mathrm{Grazing}_{\mathrm{detritus}(j,x)} \times \mathrm{POP}_{(x)}/\mathrm{POC}_{(x)}{}^{*} \times f_{\mathrm{temperature}(j,x)} \times \mathrm{ZOOP}_{(j,x)}$$
$$- \mathrm{VP}_{\mathrm{settling}} \times f_{\mathrm{temperature}(x)} \times \mathrm{POP}_{(x)} \times f_{\mathrm{depth}(x)}$$
$$+ \sum_{j=\mathrm{cop,clad}} \mathrm{FE}_{\mathrm{POP}(j)} \times \mathrm{Pegestion}_{(j,x)} - \mathrm{outflows} \times \mathrm{POP}_{(\mathrm{EPI})} + \mathrm{POP}_{\mathrm{EXOG(EPI)}}$$

$$\mathrm{Pegestion}_{(j,x)} = \left(\sum_{i=\mathrm{diat,green,cyan}} \mathrm{Grazing}_{(i,j,x)} \times P_{(i,x)} + \mathrm{Grazing}_{\mathrm{detritus}(j,x)} \times \mathrm{POP}_{(x)}/\mathrm{POC}_{(x)}{}^{*} \right)$$
$$\times (1 - \mathrm{gref}_{(j,x)}) \times f_{\mathrm{temperature}(j,x)} \times \mathrm{ZOOP}_{(j,x)}$$
$$^{*}\text{For copepods if } \frac{\mathrm{POC}_{(x)}}{\mathrm{POP}_{(x)}} > C : P_0 \text{ then } 1/C : P_0$$

A.5. Carbon

A.5.1. Dissolved organic carbon

$$\frac{\partial \mathrm{DOC}_{(x)}}{\partial t} = \sum_{i} \left[\mathrm{FBM}_{\mathrm{DOC}(i)} + (1 - \mathrm{FBM}_{\mathrm{OC}(i)}) \times \frac{\mathrm{KH}_{\mathrm{EXUD}(i)}}{\mathrm{KH}_{\mathrm{EXUD}(i)} + \mathrm{DO}_{(x)}} \right] \times \mathrm{bm}_{\mathrm{ref}(i)} \mathrm{e}^{\mathrm{ktbm}_{(i)}(T(x)-\mathrm{Tref}(i))}$$
$$\times \mathrm{PHYT}_{(i,x)} + \sum_{j} [\mathrm{FBM}_{\mathrm{DOC}(j)} + (1 - \mathrm{FBM}_{\mathrm{OC}(j)}) \times \frac{\mathrm{KH}_{\mathrm{EXUD}(j)}}{\mathrm{KH}_{\mathrm{EXUD}(j)} + \mathrm{DO}_{(x)}}]$$
$$\times \mathrm{bm}_{\mathrm{ref}(j)} \mathrm{e}^{\mathrm{ktbm}(j)(T(x)-\mathrm{Tref}(j))} \times \mathrm{ZOOP}_{(j,x)} + \sum_{j=\mathrm{cop,clad}} \mathrm{FE}_{\mathrm{DOC}} \times \mathrm{Cegestion}_{(j,x)}$$

$$- \frac{\mathrm{DO}_{(x)}}{\mathrm{DO}_{(x)} + \mathrm{KH}_{\mathrm{OOXRESP}}} \times K_{\mathrm{respdoc}(x)} \times \mathrm{DOC}_{(x)} + \mathrm{KC}_{\mathrm{dissolution}(x)} \times \mathrm{POC}_{(x)} - \mathrm{denitrification}_{(x)} / \mathrm{DENIT}_{\frac{\mathrm{NO_3}}{\mathrm{DOC}}} - \mathrm{outflows} \times \mathrm{DOC}_{(\mathrm{EPI})} \pm \mathrm{EPI}/\mathrm{YPO}_{\mathrm{DOC}} + \mathrm{DOC}_{\mathrm{EXOG(EPI)}} + \mathrm{DOC}_{\mathrm{ENDOG}(x)}$$

$$\mathrm{KC}_{\mathrm{dissolution}(x)} = \mathrm{KC}_{\mathrm{ref}_{\mathrm{dissolution}}} \times f_{\mathrm{temperature}(x)}$$

$$K_{\mathrm{respdoc}(x)} = K_{\mathrm{ref}_{\mathrm{respdoc}}} \times f_{\mathrm{temperature}(x)}$$

$$\mathrm{FM}_{\mathrm{OC}(i),(j)} = \mathrm{FM}_{\mathrm{POC}(i),(j)} + \mathrm{FM}_{\mathrm{DOC}(i),(j)}$$

A.5.2. Particulate organic carbon

$$\frac{\partial \mathrm{POC}_{(x)}}{\partial t} = \sum_{i=\mathrm{diat,green,cyan}} \mathrm{FBM}_{\mathrm{POC}(i)} \times \mathrm{bm}_{\mathrm{ref}(i)} \mathrm{e}^{\mathrm{ktbm}(i)(T(x)-\mathrm{Tref}(i))} \times \mathrm{PHYT}_{(i,x)} + \sum_{j=\mathrm{cop,clad}} \mathrm{FBM}_{\mathrm{POC}(j)} \times \mathrm{bm}_{\mathrm{ref}(j)} \mathrm{e}^{\mathrm{ktbm}(j)(T(x)-\mathrm{Tref}(j))} \times \mathrm{ZOOP}_{(j,x)} - \mathrm{KC}_{\mathrm{dissolution}(x)} \times \mathrm{POC}_{(x)} - \sum_{j=\mathrm{cop,clad}} \mathrm{Grazing}_{\mathrm{detritus}(j,x)} \times f_{\mathrm{temperature}(j,x)} \times \mathrm{ZOOP}_{(j,x)} - \mathrm{VP}_{\mathrm{settling}} \times f_{\mathrm{temperature}(x)} \times \mathrm{POC}_{(x)} \times f_{\mathrm{depth}(x)} + \sum_{j=\mathrm{cop,clad}} \mathrm{FE}_{\mathrm{POC}(j)} \times \mathrm{Cegestion}_{(j,x)} - \mathrm{outflows} \times \mathrm{POC}_{(\mathrm{EPI})} + \mathrm{POC}_{\mathrm{EXOG(EPI)}}$$

$$\mathrm{Cegestion}_{(j,x)} = \left[\left(\sum_{i=\mathrm{diat,green,cyan}} \mathrm{Grazing}_{(i,j,x)} + \mathrm{Grazing}_{\mathrm{detritus}(j,x)} \right) - C/P_{(j)} \times \mathrm{gref}_{(j,x)} \times \left(\sum_{i=\mathrm{diat,green,cyan}} \mathrm{Grazing}_{(i,j,x)} \times P_{(i,x)} + \mathrm{Grazing}_{\mathrm{detritus}(j,x)} \times \mathrm{POP}_{(x)}/\mathrm{POC}_{(x)}{}^{*} \right) \right] \times f_{\mathrm{temperature}(j,x)} \times \mathrm{ZOOP}_{(j,x)}$$

*For copepods if $\frac{\mathrm{POC}_{(x)}}{\mathrm{POP}_{(x)}} > C : P_0$ then $1/C : P_0$

A.6. Dissolved oxygen

$$\frac{\partial \mathrm{DO}_{(x)}}{\partial t} = \sum_{i=\mathrm{diat,green,cyan}} (1.3 - 0.3 \times \mathrm{prefNH_4}) \times \mathrm{growth}_{(i,x)} \times \mathrm{RESP}_{\mathrm{DO/C}} \times \mathrm{PHYT}_{(i,x)} - \sum_i \frac{\mathrm{DO}_{(x)}}{\mathrm{KH}_{\mathrm{EXUD}(i)} + \mathrm{DO}_{(x)}} \times \mathrm{bm}_{\mathrm{ref}(i)} \mathrm{e}^{\mathrm{ktbm}_{(i)}(T(x)-\mathrm{Tref}(i))} \times \mathrm{RESP}_{\mathrm{DO/C}} \times \mathrm{PHYT}_{(i,x)} - \sum_j \frac{\mathrm{DO}_{(x)}}{\mathrm{KH}_{\mathrm{EXUD}(j)} + \mathrm{DO}_{(x)}} \times \mathrm{bm}_{\mathrm{ref}(j)} \mathrm{e}^{\mathrm{ktbm}_{(j)}(T(x)-\mathrm{Tref}(j))} \times \mathrm{RESP}_{\mathrm{DO/C}} \times \mathrm{ZOOP}_{(j,x)} - \frac{\mathrm{DO}_{(x)}}{\mathrm{DO}_{(x)} + \mathrm{KH}_{\mathrm{OOXRESP}}} \times K_{\mathrm{respdoc}(x)} \times \mathrm{RESP}_{\mathrm{DO/C}} \times \mathrm{DOC}_{(x)} - \mathrm{nitrification}_{(x)} \times \mathrm{NITRIF}_{\mathrm{O/NH_4}} + \frac{K_{\mathrm{reaeration}} \times \mathrm{Surface\ area}}{\mathrm{Epilimnion\ Volume}} \times (\mathrm{DO_S} - \mathrm{DO}_{(\mathrm{epi})}) \pm \mathrm{EPI}/\mathrm{YPO}_{\mathrm{DO}} - \mathrm{DO}_{\mathrm{ENDOG}(x)}$$

$$DO_s = 14.5532 - 0.38217 \times T_{(EPI)} + 0.0054258 \times T_{(EPI)}^2 - Cl \times (1.665 \times 10^{-4} - 5.866 \times 10^{-6} \times T_{(EPI)} + 9.796 \times 10^{-8} \times T_{(EPI)}^2)$$

Cl: chloride concentration (ppt) based on values by Rattray et al. (1954).

A.7. Silica

A.7.1. Dissolved available silica

$$\frac{\partial DSi_{(x)}}{\partial t} = -Si_{up(diat,x)} \times Si_{fb(diat,x)} \times PHYT_{(diat,x)} + FBM_{DSi(diat)} \times Si_{(diat,x)} \times bm_{ref(diat)} e^{ktbm(diat)(T(x)-Tref(diat))} \times PHYT_{(diat,x)} + KSi_{dissolution(x)} \times PSi_{(x)} - outflows \times DSi_{(EPI)} \pm EPI/YPO_{DSi} + DSi_{EXOG(EPI)} + DSi_{ENDOG(x)}$$

$$KSi_{dissolution(x)} = KSi_{ref_{dissolution}} \times f_{temperature(x)}$$

A.7.2. Particulate silica

$$\frac{\partial PSi_{(x)}}{\partial t} = FBM_{PSi(diat)} \times Si_{(diat,x)} \times bm_{ref(diat)} e^{ktbm(diat)(T(x)-Tref(diat))} \times PHYT_{(diat,x)} - VPSi_{settling} \times f_{temperature(x)} \times PSi_{(x)} \times f_{depth(x)} - KSi_{dissolution(x)} \times PSi_{(x)} - outflows \times PSi_{(EPI)} + PSi_{EXOG(EPI)}$$

A.8. Sediment submodel

The terms with subscript ENDOG (sediment contribution to the water-column concentrations) are derived from the following sediment submodel.

$$DO_{SED(x)} = a_{Crel} SOC_{osed} e^{ktsed(T(x)-Tsref)}, \quad NO_{3SED(x)} = a_{NO_3rel} NO_{3osed} e^{ktsed(T(x)-Tsref)},$$
$$NH_{4SED(x)} = a_{NH_4rel} NH_{4osed} e^{ktsed(T(x)-Tsref)}, \quad PO_{4SED(x)} = a_{Prel} PO_{4osed} e^{ktsed(T(x)-Tsref)}$$

$$\frac{dSOC_{osed}}{dt} = (1 - \beta_C) \times \left[\alpha_{epi} \left(\sum_{i=diat,green,cyan} V_{settling(i)} \times f_{temperature(epi)} \times PHYT_{(i,epi)} + VP_{settling} \times f_{temperature(epi)} \times POC_{(epi)} \right) + \alpha_{hypo} \left(\sum_{i=diat,green,cyan} V_{settling(i)} \times f_{temperature(hypo)} \times PHYT_{(i,hypo)} + VP_{settling} \times f_{temperature(hypo)} \times POC_{(hypo)} \right) \right] + (\alpha_{epi} DO_{SED(epi)} + \alpha_{hypo} DO_{SED(hypo)})$$

$$\frac{\mathrm{dNH_{4osed}}}{\mathrm{d}t} = (1-\beta_{\mathrm{N}}) \times \left[\alpha_{\mathrm{epi}}\left(\sum_{i=\mathrm{diat,green,cyan}} V_{\mathrm{settling}(i)} \times f_{\mathrm{temperature(epi)}} \times N_{(i,\mathrm{epi})} \times \mathrm{PHYT}_{(i,\mathrm{epi})} + \mathrm{VP_{settling}} \times f_{\mathrm{temperature(epi)}} \times \mathrm{PON_{(epi)}}\right) + \alpha_{\mathrm{hypo}}\left(\sum_{i=\mathrm{diat,green,cyan}} V_{\mathrm{settling}(i)} \times f_{\mathrm{temperature(hypo)}} \times N_{(i,\mathrm{hypo})} \times \mathrm{PHYT}_{(i,\mathrm{hypo})} + \mathrm{VP_{settling}} \times f_{\mathrm{temperature(hypo)}} \times \mathrm{PON_{(hypo)}}\right)\right] - (\alpha_{\mathrm{epi}}\mathrm{NH_{4SED(epi)}} + \alpha_{\mathrm{hypo}}\mathrm{NH_{4SED(hypo)}}) - \mathrm{Nitrif_{sed}} \times \mathrm{NH_{4osed}}$$

$$\frac{\mathrm{dNO_{3osed}}}{\mathrm{d}t} = \mathrm{Nitrif_{sed}} \times \mathrm{NH_{4osed}} - (\alpha_{\mathrm{epi}}\mathrm{NO_{3SED(epi)}} + \alpha_{\mathrm{hypo}}\mathrm{NO_{3SED(hypo)}})$$

$$\frac{\mathrm{dPO_{4osed}}}{\mathrm{d}t} = (1-\beta_{\mathrm{P}}) \times \left[\alpha_{\mathrm{epi}}\left(\sum_{i=\mathrm{diat,green,cyan}} V_{\mathrm{settling}(i)} \times f_{\mathrm{temperature(epi)}} \times P_{(i,\mathrm{epi})} \times \mathrm{PHYT}_{(i,\mathrm{epi})} + \mathrm{VP_{settling}} \times f_{\mathrm{temperature(epi)}} \times \mathrm{POP_{(epi)}}\right) + \alpha_{\mathrm{hypo}}\left(\sum_{i=\mathrm{diat,green,cyan}} V_{\mathrm{settling}(i)} \times f_{\mathrm{temperature(hypo)}} \times P_{(i,\mathrm{hypo})} \times \mathrm{PHYT}_{(i,\mathrm{hypo})} + \mathrm{VP_{settling}} \times f_{\mathrm{temperature(hypo)}} \times \mathrm{POP_{(hypo)}}\right)\right] - (\alpha_{\mathrm{epi}}\mathrm{PO_{4SED(epi)}} + \alpha_{\mathrm{hypo}}\mathrm{PO_{4SED(hypo)}})$$

β_{C}, β_{N}, β_{P}: fractions of inert carbon (0.25), nitrogen (0.5), and phosphorus (0.5) buried into the deeper sediment layers; $\mathrm{Nitrif_{sed}}$: sediment nitrification rate ($0.75\,\mathrm{day}^{-1}$); a_{Crel}, $a_{\mathrm{NH_4rel}}$, a_{Prel}: sediment oxygen consumption, ammonium and phosphate release rates ($0.5\ \mathrm{day}^{-1}$); $a_{\mathrm{NO_3rel}}$: nitrate release rate ($1\ \mathrm{day}^{-1}$); ktsed: effects of temperature on sediment–water fluxes ($0.04\,\mathrm{C}^{\circ -1}$); Tsref: the reference temperature ($10\,^{\circ}\mathrm{C}$); and $a_{\mathrm{epi,hypo}}$: the epilimnion/hypolimnion to lake volume ratio.

The model also accounts for temperature effects on user-specified sediment–water fluxes of $\mathrm{DOC_{osed}}$, $\mathrm{DON_{osed}}$, $\mathrm{DOP_{osed}}$, and $\mathrm{DSi_{osed}}$ at the reference temperature of $10\,^{\circ}\mathrm{C}$.

$$\mathrm{DOC_{SED}}(x) = \mathrm{DOC_{osed}}\mathrm{e}^{\mathrm{ktsed}(T(x)-\mathrm{Tsref})}, \qquad \mathrm{DON_{SED}}(x) = \mathrm{DON_{osed}}\mathrm{e}^{\mathrm{ktsed}(T(x)-\mathrm{Tsref})},$$
$$\mathrm{DOP_{SED}}(x) = \mathrm{DOP_{osed}}\mathrm{e}^{\mathrm{ktsed}(T(x)-\mathrm{Tsref})}, \qquad \mathrm{DSi_{SED}}(x) = \mathrm{DSi_{osed}}\mathrm{e}^{\mathrm{ktsed}(T(x)-\mathrm{Tsref})}$$

$$\mathrm{DOC_{osed}} = 10\,\mathrm{mg\,m^{-2}\,day^{-1}}, \qquad \mathrm{DON_{osed}} = 0.5\,\mathrm{mg\,m^{-2}\,day^{-1}},$$
$$\mathrm{DOP_{osed}} = 0.1\,\mathrm{mg\,m^{-2}\,day^{-1}}, \qquad \mathrm{DSi_{osed}} = 70\,\mathrm{mg\,m^{-2}\,day^{-1}}$$

Appendix B. Description and calibration values of model parameters

Symbol	Description	References	Values	Units
$growth_{max(diat)}$	Maximum growth for diatoms	Hamilton and Schladow (1997, and references therein), Cerco and Cole (1994, and references therein), Omlin et al. (2001b), Jorgensen et al. (1991), Reynolds (1984), Chen et al. (2002, and references therein)	2.2	day^{-1}
$growth_{max(greens)}$	Maximum growth for greens	Hamilton and Schladow (1997, and references therein), Cerco and Cole (1994, and references therein), Omlin et al. (2001b), Jorgensen et al. (1991), Reynolds (1984), Chen et al. (2002, and references therein)	1.8	day^{-1}
$growth_{max(cyan)}$	Maximum growth for cyanobacteria	Hamilton and Schladow (1997, and references therein), Cerco and Cole (1994, and references therein), Omlin et al. (2001b), Jorgensen et al. (1991), Reynolds (1984), Chen et al. (2002, and references therein)	1.2	day^{-1}
$bm_{ref(diat)}$	Basal metabolism rate for diatoms	Hamilton and Schladow (1997, and references therein), Cerco and Cole (1994, and references therein), Omlin et al. (2001b), Jorgensen et al. (1991), Reynolds (1984)	0.10	day^{-1}
$bm_{ref(greens)}$	Basal metabolism rate for greens	Hamilton and Schladow (1997, and references therein), Cerco and Cole (1994, and references therein), Omlin et al. (2001b), Jorgensen et al. (1991), Reynolds (1984)	0.08	day^{-1}
$bm_{ref(cyan)}$	Basal metabolism rate for cyanobacteria	Hamilton and Schladow (1997, and references therein), Cerco and Cole (1994, and references therein), Omlin et al. (2001b), Jorgensen et al. (1991), Reynolds (1984)	0.08	day^{-1}
$ktbm_{(i)}$	Effects of temperature on phytoplankton metabolism	Cerco and Cole (1994, and references therein), Omlin et al. (2001b), Jorgensen et al. (1991), Reynolds (1984)	0.069	$C^{\circ -1}$
$Tref_{(i)}$	Reference temperature for phytoplankton metabolism	Cerco and Cole (1994, and references therein), Omlin et al. (2001b), Jorgensen et al. (1991), Reynolds (1984)	20	C°
$KN_{(diat)}$	Half saturation constant for nitrogen uptake by diatoms	Hamilton and Schladow (1997, and references therein), Cerco and Cole (1994, and references therein), Jorgensen et al. (1991), Reynolds (1984)	65	$mg\,N\,m^{-3}$
$KN_{(greens)}$	Half saturation constant for nitrogen uptake by greens	Hamilton and Schladow (1997, and references therein), Cerco and Cole (1994, and references therein), Jorgensen et al. (1991), Reynolds (1984)	45	$mg\,N\,m^{-3}$
$KN_{(cyan)}$	Half saturation constant for nitrogen uptake by cyanobacteria	Hamilton and Schladow (1997, and references therein), Cerco and Cole (1994, and references therein), Jorgensen et al. (1991), Reynolds (1984)	25	$mg\,N\,m^{-3}$

$KP_{(diat)}$	Half saturation constant for phosphorus uptake by diatoms	Hamilton and Schladow (1997, and references therein), Cerco and Cole (1994, and references therein), Omlin et al. (2001b), Jorgensen et al. (1991), Reynolds (1984), Chen et al. (2002, and references therein)	6	mg P m^{-3}
$KP_{(greens)}$	Half saturation constant for phosphorus uptake by greens	Hamilton and Schladow (1997, and references therein), Cerco and Cole (1994, and references therein), Omlin et al. (2001b), Jorgensen et al. (1991), Reynolds (1984), Chen et al. (2002, and references therein)	10	mg P m^{-3}
$KP_{(cyan)}$	Half saturation constant for phosphorus uptake by cyanobacteria	Hamilton and Schladow (1997, and references therein), Cerco and Cole (1994, and references therein), Omlin et al. (2001b), Jorgensen et al. (1991), Reynolds (1984), Chen et al. (2002, and references therein)	18	mg P m^{-3}
$KSi_{(diat)}$	Half saturation constant for silica uptake by diatoms	Jorgensen et al. (1991), Sandgren (1991), Chen et al. (2002, and references therein)	40	mg Si m^{-3}
$D_{opt(i)}$	Depth of maximum algal production	Cerco and Cole (1994, and references therein), Reynolds (1984)	1	m
$I_{o(diat)}$	Effects of light attenuation for diatom growth		1	–
$I_{o(greens)}$	Effects of light attenuation for green growth		1	–
$I_{o(cyan)}$	Effects of light attenuation for cyanobacteria growth		0.6	–
$K_{EXTback}$	Background light attenuation	Hamilton and Schladow (1997, and references therein)	0.29	m^{-1}
$K_{EXTchla}$	Light attenuation coefficient for chlorophyll	Hamilton and Schladow (1997, and references therein)	0.02	m^2 mg^{-1}
$C/chl_{(i)}$	Carbon to chlorophyll ratio for phytoplankton	Hamilton and Schladow (1997, and references therein), Reynolds (1984), Wetzel (2001), Chen et al. (2002, and references therein)	50	mg C mg chl^{-1}
$Topt_{(i)}$	Optimal temperature for phytoplankton growth	Cerco and Cole (1994, and references therein), Omlin et al. (2001b), Jorgensen et al. (1991), Reynolds (1984)	20	C°
$KTgr1_{(diat)}$	Effect of temperature below Topt for diatoms	Cerco and Cole (1994, and references therein), Omlin et al. (2001b), Jorgensen et al. (1991), Reynolds (1984)	0.004	$C^{\circ -2}$
$KTgr2_{(diat)}$	Effect of temperature above Topt for diatoms	Cerco and Cole (1994, and references therein), Omlin et al. (2001b), Jorgensen et al. (1991), Reynolds (1984)	0.004	$C^{\circ -2}$
$KTgr1_{(greens)}$	Effect of temperature below Topt for greens	Cerco and Cole (1994, and references therein), Omlin et al. (2001b), Jorgensen et al. (1991), Reynolds (1984)	0.005	$C^{\circ -2}$
$KTgr2_{(greens)}$	Effect of temperature above Topt for greens	Cerco and Cole (1994, and references therein), Omlin et al. (2001b), Jorgensen et al. (1991), Reynolds (1984)	0.005	$C^{\circ -2}$
$KTgr1_{(cyan)}$	Effect of temperature below Topt for cyanobacteria	Cerco and Cole (1994, and references therein), Omlin et al. (2001b), Jorgensen et al. (1991), Reynolds (1984)	0.006	$C^{\circ -2}$
$KTgr2_{(cyan)}$	Effect of temperature above Topt for cyanobacteria	Cerco and Cole (1994, and references therein), Omlin et al. (2001b), Jorgensen et al. (1991), Reynolds (1984)	0.006	$C^{\circ -2}$
$V_{settling(diat)}$	Settling velocity for diatoms at reference temperature	Cerco and Cole (1994, and references therein), Reynolds (1984), Sandgren (1991), Wetzel (2001)	0.35	m day^{-1}
$V_{settling(greens)}$	Settling velocity for greens at reference temperature	Cerco and Cole (1994, and references therein), Reynolds (1984), Sandgren (1991), Wetzel (2001)	0.25	m day^{-1}

Symbol	Description	References	Values	Units
$V_{\text{settling(cyano)}}$	Settling velocity for cyanobacteria at reference temperature	Cerco and Cole (1994, and references therein), Reynolds (1984), Sandgren (1991), Wetzel (2001)	0.02	m day^{-1}
$\psi_{(i)}$	Strength of the ammonium preference		0.3	$(\text{mg N m}^{-3})^{-1}$
$\text{grazing}_{\text{max(clad)}}$	Maximum grazing rate for cladocerans	Jorgensen et al. (1991), Lampert and Sommer (1997), Wetzel (2001), Sommer (1989), Chen et al. (2002, and references therein)	0.8	day^{-1}
$\text{grazing}_{\text{max(cop)}}$	Maximum grazing rate for copepods	Jorgensen et al. (1991), Lampert and Sommer (1997), Wetzel (2001), Sommer (1989), Chen et al. (2002, and references therein)	0.45	day^{-1}
$\text{KZ}_{\text{(clad)}}$	Half saturation constant for grazing by cladocerans	Jorgensen et al. (1991), Sommer (1989)	120	mg C m^{-3}
$\text{KZ}_{\text{(cop)}}$	Half saturation constant for grazing by copepods	Jorgensen et al. (1991), Sommer (1989)	100	mg C m^{-3}
$\text{pref}_{\text{(diat,clad)}}$	Preference of cladocerans for diatoms		0.25	–
$\text{pref}_{\text{(greens,clad)}}$	Preference of cladocerans for greens		0.25	–
$\text{pref}_{\text{(cyano,clad)}}$	Preference of cladocerans for cyanobacteria		0.25	–
$\text{pref}_{\text{det(clad)}}$	Preference of cladocerans for detritus		0.25	–
$\text{pref}_{\text{(diat,cop)}}$	Preference of copepods for diatoms		0.30	–
$\text{pref}_{\text{(greens,cop)}}$	Preference of copepods for greens		0.25	–
$\text{pref}_{\text{(cyano,cop)}}$	Preference of copepods for cyanobacteria		$0.45 - \text{pref}_{\text{(det,cop)}}$	–
$\text{pref}_{\text{det(cop)}}$	Preference of copepods for detritus		[a]	–
$\text{FQ}_{\text{(diat,}j\text{)}}$	Quality as a food of diatoms	Brett et al. (2000 and references therein), Park et al. (2002)	0.9	–
$\text{FQ}_{\text{(greens,}j\text{)}}$	Quality as a food of greens	Brett et al. (2000 and references therein), Park et al. (2002)	0.7	–
$\text{FQ}_{\text{(cyano,}j\text{)}}$	Quality as a food of cyanobacteria	Brett et al. (2000 and references therein), Park et al. (2002)	0.1	–
$\text{FQ}_{\text{det(}j\text{)}}$	Quality as a food of detritus	Brett et al. (2000 and references therein), Park et al. (2002), Ederington et al. (1995)	0.5	–
$C{:}P_0$	Critical threshold for mineral P limitation	Brett et al. (2000 and references therein)	100	
$\text{ef}_{1(j)}$	Specific zooplankton growth efficiency for phosphorus	Sterner and Hessen (1994)	1	–
$\text{ef}_{2\text{(clad)}}$	Half saturation constant for cladocerans growth efficiency		18	$(\text{mg C m}^{-3})^{1/2}$

$ef_{2(cop)}$	Half saturation constant for copepods growth efficiency		20	$(mg\,C\,m^{-3})^{1/2}$
$pred_1$	Specific zooplankton predation rate	Fasham (1993), Ross et al. (1994), Malchow (1994)	0.15	day^{-1}
$pred_2$	Half saturation constant for predation	Fasham (1993), Ross et al. (1994), Malchow (1994)	40	$mg\,C\,m^{-3}$
$bm_{ref(clad)}$	Cladocerans basal metabolism rate	Omlin et al. (2001b), Jorgensen et al. (1991), Lampert and Sommer (1997), Wetzel (2001), Sommer (1989), Chen et al. (2002, and references therein)	0.05	day^{-1}
$ktbm_{(clad)}$	Effects of temperature on cladocerans metabolism	Omlin et al. (2001b), Wetzel (2001)	0.10	$C^{\circ -1}$
$bm_{ref(cop)}$	Copepods basal metabolism rate	Omlin et al. (2001b), Jorgensen et al. (1991), Lampert and Sommer (1997), Wetzel (2001), Sommer (1989), Chen et al. (2002, and references therein)	0.04	day^{-1}
$ktbm_{(cop)}$	Effects of temperature on copepods metabolism	Omlin et al. (2001b), Wetzel (2001)	0.05	$C^{\circ -1}$
$Tref_{(j)}$	Reference temperature for zooplankton	Omlin et al. (2001b), Lampert and Sommer (1997), Wetzel (2001), Downing and Rigler (1984), Orcutt and Porter (1983)	20	C°
$Topt_{(clad)}$	Optimal temperature for cladoceran growth grazing	Omlin et al. (2001b), Lampert and Sommer (1997), Wetzel (2001), Downing and Rigler (1984), Orcutt and Porter (1983)	20	C°
$KTgr1_{(clad)}$	Effect of temperature below Topt for cladocerans	Omlin et al. (2001b), Lampert and Sommer (1997), Wetzel (2001), Downing and Rigler (1984), Orcutt and Porter (1983)	0.015	$C^{\circ -2}$
$KTgr2_{(clad)}$	Effect of temperature above Topt for cladocerans	Omlin et al. (2001b), Lampert and Sommer (1997), Wetzel (2001), Downing and Rigler (1984), Orcutt and Porter (1983)	0.015	$C^{\circ -2}$
$Topt_{(cop)}$	Optimal temperature for copepod growth grazing	Omlin et al. (2001b), Lampert and Sommer (1997), Wetzel (2001), Downing and Rigler (1984), Orcutt and Porter (1983)	18	C°
$KTgr1_{(cop)}$	Effect of temperature below Topt for copepods	Omlin et al. (2001b), Lampert and Sommer (1997), Wetzel (2001), Downing and Rigler (1984), Orcutt and Porter (1983)	0.002	$C^{\circ -2}$
$KTgr2_{(cop)}$	Effect of temperature above Topt for copepods	Omlin et al. (2001b), Lampert and Sommer (1997), Wetzel (2001), Downing and Rigler (1984), Orcutt and Porter (1983)	0.002	$C^{\circ -2}$
$N_{upmax(i)}$	Maximum nitrogen uptake rate	Hamilton and Schladow (1997, and references therein), Jorgensen et al. (1991)	0.16	$mg\,N\,mg\,C^{-1}\,day^{-1}$
$N_{max(i)}$	Maximum phytoplankton internal N	Hamilton and Schladow (1997, and references therein), Jorgensen et al. (1991)	0.18	$mg\,N\,mg\,C^{-1}$
$N_{min(i)}$	Minimum phytoplankton internal N	Hamilton and Schladow (1997, and references therein), Jorgensen et al. (1991)	0.08	$mg\,N\,mg\,C^{-1}$
$P_{upmax(i)}$	Maximum phosphorus uptake rate	Hamilton and Schladow (1997, and references therein), Jorgensen et al. (1991)	0.009	$mg\,P\,mg\,C^{-1}\,day^{-1}$

Symbol	Description	References	Values	Units
$P_{max(i)}$	Maximum phytoplankton internal P	Hamilton and Schladow (1997, and references therein), Jorgensen et al. (1991)	0.025	mg P mg C^{-1}
$P_{min(i)}$	Minimum phytoplankton internal P	Hamilton and Schladow (1997, and references therein), Jorgensen et al. (1991)	0.008	mg P mg C^{-1}
$Si_{upmax(i)}$	Maximum silica uptake rate	Jorgensen et al. (1991), Sandgren (1991)	0.35	mg Si mg C^{-1} day^{-1}
$Si_{max(i)}$	Maximum phytoplankton internal Si	Jorgensen et al. (1991), Teubner and Dokulil (2002), Conley et al. (1989)	0.40	mg Si mg C^{-1}
$Si_{min(i)}$	Minimum phytoplankton internal Si	Jorgensen et al. (1991), Teubner and Dokulil (2002), Conley et al. (1989)	0.30	mg Si mg C^{-1}
$C/N_{(clad)}$	Carbon to nitrogen ratio for cladocerans	Hessen and Lyche (1991), Sterner et al. (1992)	6	mg C mg N^{-1}
$C/N_{(cop)}$	Carbon to nitrogen ratio for copepods	Hessen and Lyche (1991), Sterner et al. (1992)	5	mg C mg N^{-1}
$C/P_{(clad)}$	Carbon to phosphorus ratio for cladocerans	Hessen and Lyche (1991), Sterner et al. (1992)	35	mg C mg P^{-1}
$C/P_{(cop)}$	Carbon to phosphorus ratio for copepods	Hessen and Lyche (1991), Sterner et al. (1992)	50	mg C mg P^{-1}
$nitrif_{max}$	Maximum nitrification rate at optimal temperature	Hamilton and Schladow (1997, and references therein), Cerco and Cole (1994, and references therein), Berounsky and Nixon (1990)	0.15	mg N m^{-3} day^{-1}
KH_{ONIT}	Half saturation concentration of DO required for nitrification	Cerco and Cole (1994, and references therein)	0.7	mg O_2 m^{-3}
KH_{NH_4NIT}	Half saturation concentration of ammonium required for nitrification	Cerco and Cole (1994, and references therein)	0.08	mg N m^{-3}
$R_{denitr/oxresp}$	Ratio of denitrification to oxic respiration rate	Cerco and Cole (1994, and references therein)	0.5	–
$KH_{OOXRESP}$	Half saturation concentration of DO required for oxic respiration	Cerco and Cole (1994, and references therein)	0.5	mg O_2 m^{-3}
KH_{NO_3DENIT}	Half saturation concentration of nitrate required for denitrification	Cerco and Cole (1994, and references therein)	0.2	mg N m^{-3}
$DENIT_{NO_3/DOC}$	Mass of nitrate–nitrogen reduced per mass DOC oxidized	Cerco and Cole (1994, and references therein)	0.933	mg N mg C^{-1}
Toptnitr	Optimal temperature for nitrification	Cerco and Cole (1994, and references therein), Berounsky and Nixon (1990)	28	C°
KT_{nitr1}	Effect of temperature below Topt for nitrification	Cerco and Cole (1994, and references therein), Berounsky and Nixon (1990)	0.002	$C^{\circ -2}$
KT_{nitr2}	Effect of temperature above Topt for nitrification	Cerco and Cole (1994, and references therein), Berounsky and Nixon (1990)	0.002	$C^{\circ -2}$
$Kref_{respDOC}$	Respiration rate of dissolved organic carbon at reference temperature	Cerco and Cole (1994, and references therein)	0.0024	day^{-1}
$KNref_{mineral}$	Nitrogen mineralization rate at reference temperature	Hamilton and Schladow (1997, and references therein), Cerco and Cole (1994, and references therein)	0.0045	day^{-1}

$KPref_{mineral}$	Phosphorus mineralization rate at reference temperature	Hamilton and Schladow (1997, and references therein), Cerco and Cole (1994, and references therein), Omlin et al. (2001b)	0.04	day^{-1}
$KCref_{dissolution}$	Particulate carbon dissolution/hydrolysis rate at reference temperature	Cerco and Cole (1994, and references therein)	0.008	day^{-1}
$KNref_{dissolution}$	Particulate nitrogen dissolution/hydrolysis rate at reference temperature	Cerco and Cole (1994, and references therein)	0.0005	day^{-1}
$KPref_{dissolution}$	Particulate phosphorus dissolution/hydrolysis rate at reference temperature	Cerco and Cole (1994, and references therein)	0.008	day^{-1}
$KSiref_{dissolution}$	Particulate silica dissolution/hydrolysis rate at reference temperature	Cerco and Cole (1994, and references therein)	0.008	day^{-1}
Tref	Reference temperature for biological processes		20	C°
KT1	Effect of temperature below Tref		0.004	$C^{\circ -2}$
KT2	Effect of temperature above Tref		0.004	$C^{\circ -2}$
$K_{rearation}$	Reaeration coefficient	Cerco and Cole (1994, and references therein)	2.4	$m\,day^{-1}$
$VP_{settling}$	Settling velocity of particles at reference temperature	Cerco and Cole (1994, and references therein)	0.9	$m\,day^{-1}$
$VPSi_{settling}$	Settling velocity of particulate silica at reference temperature	Cerco and Cole (1994, and references therein)	1.5	$m\,day^{-1}$
$KH_{EXUD(i),(j)}$	Half saturation concentration for DOC excretion	Cerco and Cole (1994, and references therein)	0.5	$mg\,O_2\,m^{-3}$
$NITRIF_{O/NH_4}$	Mass of dissolved oxygen consumed per mass ammonium-nitrogen nitrified	Cerco and Cole (1994, and references therein)	4.33	$mg\,O_2\,mg\,N^{-1}$
$RESP_{DO/C}$	Dissolved oxygen to carbon ratio in respiration	Cerco and Cole (1994, and references therein)	2.67	$mg\,O_2\,mg\,C^{-1}$
$FBM_{NH_4(i),(j)}$	Fraction of basal metabolism excreted as ammonium	Cerco and Cole (1994, and references therein)	0.25	–
$FE_{NH_4(j)}$	Fraction of ammonium egested during zooplankton feeding		0.25	–
$FBM_{DON(i),(j)}$	Fraction of basal metabolism excreted as DON	Cerco and Cole (1994, and references therein)	0.10	–
$FE_{DON(j)}$	Fraction of DON egested during zooplankton feeding		0.10	–
$FBM_{PON(i),(j)}$	Fraction of basal metabolism excreted as PON	Cerco and Cole (1994, and references therein)	0.65	–
$FE_{PON(j)}$	Fraction of PON egested during zooplankton feeding		0.65	–
$FBM_{PO_4(i),(j)}$	Fraction of basal metabolism excreted as phosphate	Cerco and Cole (1994, and references therein)	0.20	–

Symbol	Description	References	Values	Units
$FE_{PO_4(j)}$	Fraction of phosphate egested during zooplankton feeding		0.20	–
$FBM_{DOP(i),(j)}$	Fraction of basal metabolism excreted as DOP	Cerco and Cole (1994, and references therein)	0.35	–
$FE_{DOP(j)}$	Fraction of DOP egested during zooplankton feeding		0.35	–
$FBM_{POP(i),(j)}$	Fraction of basal metabolism excreted as POP	Cerco and Cole (1994, and references therein)	0.45	–
$FE_{POP(j)}$	Fraction of POP egested during zooplankton feeding		0.45	–
$FBM_{DOC(i),(j)}$	Fraction of basal metabolism excreted as DOC	Cerco and Cole (1994, and references therein)	0.20	–
$FE_{DOC(j)}$	Fraction of DOC egested during zooplankton feeding		0.20	–
$FBM_{POC(i),(j)}$	Fraction of basal metabolism excreted as POC	Cerco and Cole (1994, and references therein)	0.50	–
$FE_{POC(j)}$	Fraction of POC egested during zooplankton feeding		0.50	–
$FBM_{Dsi(diat)}$	Fraction of basal metabolism of diatoms excreted as DSi	Cerco and Cole (1994, and references therein)	0.50	–
$FBM_{Psi(diat)}$	Fraction of basal metabolism of diatoms excreted as PSi	Cerco and Cole (1994, and references therein)	0.50	–

[a] If $\frac{POC_{(x)}}{POP_{(x)}} < C{:}P_0$, then 0.30, else $0.30 \times C/P_{LIM(x)}$.

References

Ahlgren, G., Lundstedt, L., Brett, M.T., Forsberg, C., 1990. Lipid composition and food quality of some freshwater phytoplankton for cladoceran zooplankters. J. Plankton Res. 12, 809–818.

Ahlgren, I., Frisk, T., Kamp-Nielsen, L., 1988. Empirical and theoretical-models of phosphorus loading, retention and concentration vs. lake trophic state. Hydrobiologia 170, 285–303.

Andersen, T., Hessen, D.O., 1991. Carbon, nitrogen, and phosphorus-content of freshwater zooplankton. Limnol. Oceanogr. 36, 807–814.

Anson, J.M., Schindler, D.E., Scheuerell, M.D., Fresh, K.L., Litt, A.H., Shepherd, J.H., Sibley, T.H., 2002. Planktivore diet switching and zooplankton community dynamics. In: American Society of Limnology and Oceanography Summer Meeting, Victoria, British Columbia, Canada, 10–14 June.

Arhonditsis, G., Tsirtsis, G., Karydis, M., 2002. The effects of episodic rainfall events to the dynamics of coastal marine ecosystems: applications to a semi-enclosed gulf in the Mediterranean Sea. J. Mar. Syst. 35, 183–205.

Arhonditsis, G., Brett, M.T., Frodge, J., 2003. Environmental control and limnological impacts of a large recurrent spring bloom in Lake Washington, USA. Environ. Manage. 31, 603–618.

Arhonditsis, G.B., Brett, M.T., De Gasperi, C.L., Schindler, D.E., 2004a. Effects of climatic variability on the thermal properties of Lake Washington (USA). Limnol. Oceanogr. 49, 256–270.

Arhonditsis, G.B., Winder, M., Brett, M.T., Schindler, D.E., 2004b. Patterns and mechanisms of phytoplankton variability in Lake Washington (USA). Water Res. 38, 4013–4027.

Asaeda, T., Van Bon, T., 1997. Modelling the effects of macrophytes on algal blooming in eutrophic shallow lakes. Ecol. Model. 104, 261–287.

Beauchamp, D.A., 1996. Estimating the carrying capacity for planktivorous fishes in Lake Washington. Washington Department of Fisheries and Wildlife.

Beck, M.B., 1987. Water-quality modeling—a review of the analysis of uncertainty. Water Resour. Res. 23, 1393–1442.

Berounsky, V.M., Nixon, S.W., 1990. Temperature and the annual cycle of nitrification in waters of Narragansett bay. Limnol. Oceanogr. 35, 1610–1617.

Brett, M.T., Müller-Navarra, D.C., 1997. The role of highly unsaturated fatty acids in aquatic foodweb processes. Freshwater Biol. 38, 483–499.

Brett, M.T., Müller-Navarra, D.C., Park, S.K., 2000. Empirical analysis of mineral P limitation's impact on algal food quality for freshwater zooplankton. Limnol. Oceanogr. 47, 1564–1575.

Brett, M.T., Arhonditsis, G.B., Mueller, S.E., Hartley, D.M., Frodge, J.D., Funke, D.E. Non point source impacts on stream nutrient concentrations along a forest to urban gradient. Environ. Manage. in press.

Brun, R., Reichert, P., Künsch, H.R., 2001. Practical identifiability analysis of large environmental simulation models. Water Resour. Res. 37, 1015–1030.

Campolongo, F., Saltelli, A., 1997. Sensitivity analysis of an environmental model an application of different analysis methods. Reliab. Eng. Syst. Safe. 57, 49–69.

Cerco, C.F., Cole, T.M., 1994. CE-QUAL-ICM: a three-dimensional eutrophication model, version 1.0. User's Guide, US Army Corps of Engineers Waterways Experiments Station, Vicksburgh, MS.

Chen, C., Ji, R., Schwab, D.J., Beletsky, D., Fahnenstiel, G.L., Jiang, M., Johengen, T.H., Vanderploeg, H., Eadie, B., Budd, J.W., Bundy, M.H., Gardner, W., Cotner, J., Lavrentyev, P.J., 2002. A model study of the coupled biological and physical dynamics in Lake Michigan. Ecol. Model. 152, 145–168.

Cole, T.M., Buchak, E., 1995. CE-QUAL-W2: A Two-dimensional, Laterally Averaged, Hydrodynamic and Water Quality Model, version 2.0. Technical Report, US Army Corps of Engineers Waterways Experiments Station, Vicksburgh, MS.

Conley, D.J., Kilham, S.S., Theriot, E., 1989. Differences in silica content between marine and freshwater diatoms. Limnol. Oceanogr. 34, 205–213.

DeMott, W.R., 1989. Optimal foraging theory as a predictor of chemically mediated food selection by suspension-feeding copepods. Limnol. Oceanogr. 34, 140–154.

Di Toro, D.M., Paquin, P.R., Subburamu, K., Gruber, D.A., 1990. Sediment oxygen demand model: methane and ammonia oxidation. J. Environ. Eng. ASCE 116, 945–986.

Dillon, P.J., Rigler, F.H., 1974. A test of a simple nutrient budget model predicting the phosphorus concentration in lake water. J. Fish Res. Board. Can. 31, 1771–1778.

Downing, J.A., Rigler, F.H., 1984. A Manual on Methods for the Assessment of Second Productivity in Fresh Water, second ed. Blackwell Scientific Publications, Oxford, UK.

Ederington, M.C., McManus, G.B., Harvey, H.R., 1995. Trophic transfer of fatty-acids, sterols and a triterpenoid alcohol between bacteria, a ciliate and the copepod *Acartia tonsa*. Limnol. Oceanogr. 40, 860–867.

Edmondson, W.T., 1997. Aphanizomenon in Lake Washington. Arch. Hydrobiol. 107 (Suppl), 409–446.

Edmondson, W.T., Lehman, J.T., 1981. The effect of changes in the nutrient income on the condition of Lake Washington. Limnol. Oceanogr. 26, 1–29.

Edmondson, W.T., Litt, A.H., 1982. *Daphnia* in Lake Washington. Limnol. Oceanogr. 27, 272–293.

Edwards, A.M., Yool, A., 2000. The role of higher predation in plankton population models. J. Plankton Res. 22, 1085–1112.

Elser, J.J., Urabe, J., 1999. The stoichiometry of consumer-driven nutrient recycling: theory, observations, and consequences. Ecology 80, 735–751.

Fasham, M.J.R., 1993. Modelling the marine biota. In: Heimann, M. (Ed.), The Global Carbon Cycle. Springer-Verlag, Berlin, pp. 457–504.

Fasham, M.J.R., Ducklow, H.W., McKelvie, S.M., 1990. A nitrogen-based model of plankton dynamics in the oceanic mixed layer. J. Mar. Res. 48, 591–639.

Ferris, J.M., Christian, R., 1991. Aquatic primary production in relation to microalgal responses to changing light—a review. Aquat. Sci. 53, 187–217.

Genet, L., Smith, D., Sonnen, M., 1974. Computer Program Documentation for the Dynamic Estuary Model. US Environmental Protection Agency, Systems Development Branch, Washington, DC.

Hamilton, D.P., Schladow, S.G., 1997. Prediction of water quality in lakes and reservoirs. Part 1. Model description. Ecol. Model. 96, 91–110.

Helton, J.C., 1993. Uncertainty and sensitivity analysis techniques for use in performance assessment for radioactive-waste disposal. Reliab. Eng. Syst. Safe. 42, 327–367.

Hessen, D.O., Lyche, A., 1991. Interspecific and intraspecific variations in zooplankton element composition. Arch. Hydrobiol. 121, 343–353.

Heuberger, P.C.S., Janssen, P.H.M., 1994. UNCSAM: a software tool for sensitivity and uncertainty analysis of mathematical models. In: Grasman, J., van Straten, G. (Eds.), Predictability and Nonlinear Modelling in Natural Sciences and Economics. Kluwer Academic Publishers, Dordrecht, pp. 362–376.

Hornberger, G.M., Spear, R.C., 1980. Eutrophication in Peel Inlet. Part I. The problem: defining behavior and a mathematical model for the phosphorus scenario. Water Res. 14, 29–42.

Infante, A., Edmondson, W.T., 1985. Edible phytoplankton and herbivorous zooplankton in Lake Washington. Arch. Hydrobiol./Beih 21, 161–171.

Janssen, P.H.M., 1994. Assessing sensitivities and uncertainties in models: a critical evaluation. In: Grasman, J., van Straten, G. (Eds.), Predictability and Nonlinear Modelling in Natural Sciences and Economics. Kluwer Academic Publishers, Dordrecht, pp. 344–361.

Jassby, A.D., Platt, T., 1976. Mathematical formulation of relationship between photosunthesis and light for phytoplankton. Limnol. Oceanogr. 21, 540–547.

Jorgensen, S.E., 1997. Integration of Ecosystem Theories: A Pattern. Kluwer Academic Publishers, Dordrecht.

Jorgensen, S.E., 1999. State-of-the-art of ecological modeling with emphasis on development of structural dynamic models. Ecol. Model. 120, 75–96.

Jorgensen, S.E., Nielsen, S.N., Jorgensen, L.A., 1991. Handbook of Ecological Parameters and Ecotoxicology. Pergamon Press, Amsterdam.

Jorgensen, S.E., Ray, S., Berec, L., Straskraba, M., 2002. Improved calibration of a eutrophication model by use of the size variation due to succession. Ecol. Model. 153, 269–277.

Karagounis, I., Trösch, J., Zamboni, F., 1993. A coupled physical–biochemical lake model for forecasting water quality. Aquat. Sci. 55, 87–102.

Kilham, S.S., Kreeger, D.A., Goulden, C.E., Lynn, S.G., 1997. Effects of algal food quality on fecundity and population growth rates of *Daphnia*. Freshwater Biol. 38, 639–647.

King County Water Quality Report, 2000. Water Quality Survey Results 2000. Department of Natural Resources, King County, Washington.

Kleppel, G.S., Burkart, C.A., Houchin, L., 1998. Nutrition and the regulation of egg production in the calanoid copepod *Acartia tonsa*. Limnol. Oceanogr. 43, 1000–1007.

Klepper, O., 1997. Multivariate aspects of model uncertainty analysis: tools for sensitivity analysis and calibration. Ecol. Model. 101, 1–13.

Kuivila, K.M., Murray, J.W., 1984. Organic-matter diagenesis in fresh-water sediments—the alkalinity and total CO_2 balance and methane production in the sediments of Lake Washington. Limnol. Oceanogr. 29, 1218–1230.

Kuivila, K.M., Murray, J.W., Devol, A.H., Lidstrom, M.E., Reimers, C.E., 1988. Methane cycling in the sediments of Lake Washington. Limnol. Oceanogr. 33, 571–581.

Lampert, W., Sommer, U., 1997. Limnoecology. Oxford University Press.

Lehman, J.T., 1978. Aspects of nutrient dynamics in freshwater communities. Ph.D. thesis. University of Washington.

Malchow, H., 1994. Non-equilibrium structures in plankton dynamics. Ecol. Model. 75, 123–134.

Meeuwig, J.J., Peters, R.H., 1996. Circumventing phosphorus in lake management: a comparison of chlorophyll a predictions from land-use and phosphorus-loading models. Can. J. Fish Aquat. Sci. 53, 1795–1806.

Menshutkin, V.V., Astrakhantsev, G.P., Yegorova, N.B., Rukhovets, L.A., Simo, T.L., Petrova, N.A., 1998. Mathematical modeling of the evolution and current conditions of the Ladoga Lake ecosystem. Ecol. Model. 107, 1–24.

Muck, P., Lampert, W., 1984. An experimental study on the importance of food conditions for the relative abundance of calanoid copepods and cladocerans. Comparative feeding studies with Eudiaptomus gracilis and *Daphnia longispina*. Archiv. für Hydrobiol. Suppl. 66, 157–179.

Müller-Navarra, D.C., Brett, M.T., Liston, A., Goldman, C.R., 2000. A highly-unsaturated fatty acid predicts biomass transfer between primary producers and consumers. Nature 403, 74–77.

Omlin, M., Reichert, P., Forster, R., 2001a. Biogeochemical model of lake Zürich: model equations and results. Ecol. Model. 141, 77–103.

Omlin, M., Brun, P., Reichert, P., 2001b. Biogeochemical model of Lake Zürich: sensitivity, identifiability and uncertainty analysis. Ecol. Model. 141, 105–123.

Orcutt, J.D., Porter, K.G., 1983. Diel vertical migration by zooplankton-constant and fluctuating temperature effects on life-history parameters of *Daphnia*. Limnol. Oceanogr. 28, 720–730.

Overland, J.E., Preisendorfer, R.W., 1982. A significance test for principal components applied to a cyclone climatology. Mon. Weather Rev. 110, 1–4.

Park, S., Brett, M.T., Müller-Navarra, D.C., Goldman, C.R., 2002. Essential fatty acid content and the phosphorus to carbon ratio in cultured algae as indicators of food quality for *Daphnia*. Freshwater Biol. 47, 1377–1390.

Pastres, R., Franco, D., Pecenik, G., Solidoro, C., Dejak, C., 1997. Local sensitivity analysis of a distributed parameters water quality model. Reliab. Eng. Syst. Safe. 57, 21–30.

Pastres, R., Chan, K., Solidoro, C., Dejak, C., 1999. Global sensitivity analysis of a shallow-water 3D eutrophication model. Comput. Phys. Commun. 117, 62–74.

Penn, M.R., Auer, M.T., VanOrman, E.L., Korienek, J.J., 1995. Phosphorus diagenesis in lake sediments: investigations using fractionation techniques. Mar. Freshwater Res. 46, 89–99.

Quay, P.D., Broecker, W.S., Hesslein, R.H., Schindler, D.W., 1980. Vertical diffusion rates determined by Tritium tracer experiments in the thermocline and hypolimnion of two lakes. Limnol. Oceanogr. 25, 201–218.

Quay, P.D., Emerson, S.R., Quay, B.M., Devol, A.H., 1986. The carbon-cycle for Lake Washington—a stable isotope study. Limnol. Oceanogr. 31, 596–611.

Rajar, R., Cetina, M., 1997. Hydrodynamic and water quality modelling: an experience. Ecol. Model. 101, 195–207.

Rattray M.Jr., Seckel, G.R., Barnes, C.A., 1954. Salt budget in the Lake Washington ship canal. J. Mar. Res. 13, 263–275.

Reckhow, K.H., Chapra, S.C., 1999. Modeling excessive nutrient loading in the environment. Environ. Pollut. 100, 197–207.

Reichert, P., Omlin, M., 1997. On the usefulness of overparameterized ecological models. Ecol. Model. 95, 289–299.

Reynolds, C.S., 1984. The Ecology of Freshwater Phytoplankton. Cambridge University Press, Cambridge, UK.

Riley, M.J., Stefan, H.G., 1988. MINLAKE: a dynamic lake water quality simulation model. Ecol. Model. 43, 155–182.

Ross, A.H., Gurney, W.S.C., Heath, M.R., 1994. A comparative study of the ecosystem dynamics of four fjords. Limnol. Oceanogr. 39, 318–343.

Sandgren, C.D., 1991. Growth and Reproductive Strategies of Freshwater Phytoplankton. Cambridge University Press.

Savchuk, O.P., 2002. Nutrient biogeochemical cycles in the Gulf of Riga: scaling up field studies with a mathematical model. J. Mar. Syst. 32, 253–280.

Sommer, U., 1989. Phytoplankton Ecology. Succession in Plankton Communities. Springer-Verlag.

Spear, R.C., 1997. Large simulation models: calibration, uniqueness and goodness of fit. Environ. Model. Softw. 12, 219–228.

Steinberg, L.J., Reckhow, K.H., Wolpert, R.L., 1997. Characterization of parameters in mechanistic models: a case study of a PCB fate and transport model. Ecol. Model. 97, 35–46.

Sterner, R.W., 1990. The ratio of nitrogen to phosphorus resupplied by herbivores—zooplankton and the algal competitive arena. Am. Nat. 136, 209–229.

Sterner, R.W., Elser, J.J., Hessen, D.O., 1992. Stoichiometric relationships among producers, consumers, and nutrient cycling in pelagic ecosystems. Biogeochemistry 17, 49–67.

Sterner, R.W., Hessen, D.O., 1994. Algal nutrient limitation and the nutrition of aquatic herbivores. Ann. Rev. Ecol. Syst. 25, 1–29.

Straile, D., 1997. Gross growth efficiencies of protozoan and metazoan zooplankton and their dependence on food concentration, predator–prey weight ration, and taxonomic group. Limnol. Oceanogr. 42, 1375–1385.

Teubner, K., Dokulil, M.T., 2002. Ecological stoichiometry of TN: TP: SRSi in freshwaters: nutrient ratios and seasonal shifts in phytoplankton assemblages. Arch. Hydrobiol. 154, 625–646.

Tian, R.C., Vezina, A.F., Starr, M., Saucier, F., 2001. Seasonal dynamics of coastal ecosystems and export production at high latitudes: a modeling study. Limnol. Oceanogr. 46, 1845–1859.

Touratier, F., Field, J.G., Moloney, C.L., 2001. A stoichiometric model relating growth substrate quality (C:N:P ratios) to N:P ratios in the products of heterotrophic release and excretion. Ecol. Model. 139, 265–291.

Vollenweider, R.A., 1975. Input–output models with special reference to the phosphorus loading concept in limnology. Schweiz. Z. Hydrol. 37, 53–84.

Walters, R.A., 1980. Time and depth-dependent model for physical, chemical and biological cycles in temperate lakes. Ecol. Model. 8, 79–96.

Wetzel, R.G., 2001. Limnology: Lake and River Ecosystems, third ed. Academic Press, New York, USA.

Wroblewski, J.S., 1977. Model of phytoplankton plume formation during variable Oregon upwelling. J. Mar. Res. 35, 357–394.

Zhang, J.J., Jorgensen, S.E., Tan, C.O., Beklioglu, M., 2003a. A structurally dynamic modelling—Lake Mogan, Turkey as a case study. Ecol. Model. 164, 103–120.

Zhang, J.J., Jorgensen, S.E., Beklioglu, M., Ince, O., 2003b. Hysteresis in vegetation shift—Lake Mogan prognoses. Ecol. Model. 164, 227–238.

Zhang, J.J., Jorgensen, S.E., Mahler, H., 2004. Examination of structurally dynamic eutrophication model. Ecol. Model. 173, 313–333.